



Delft University of Technology

## Combining the Augmented Lagrangian Preconditioner with the SIMPLE Schur Complement Approximation

He, Xin; Vuik, Cornelis; Klaij, Christiaan M.

**DOI**

[10.1137/17M1144775](https://doi.org/10.1137/17M1144775)

**Publication date**

2018

**Document Version**

Accepted author manuscript

**Published in**

SIAM Journal on Scientific Computing

**Citation (APA)**

He, X., Vuik, C., & Klaij, C. M. (2018). Combining the Augmented Lagrangian Preconditioner with the SIMPLE Schur Complement Approximation. *SIAM Journal on Scientific Computing*, 40(3), 1362-1385. <https://doi.org/10.1137/17M1144775>

**Important note**

To cite this publication, please use the final published version (if applicable). Please check the document version above.

**Copyright**

Other than for strictly personal use, it is not permitted to download, forward or distribute the text or part of it, without the consent of the author(s) and/or copyright holder(s), unless the work is under an open content license such as Creative Commons.

**Takedown policy**

Please contact us and provide details if you believe this document breaches copyrights. We will remove access to the work immediately and investigate your claim.

1                                   **COMBINING THE AUGMENTED LAGRANGIAN**  
2                                   **PRECONDITIONER WITH THE SIMPLE SCHUR COMPLEMENT**  
3                                   **APPROXIMATION\***

4                                   XIN HE<sup>†</sup>, CORNELIS VUIK<sup>‡</sup>, AND CHRISTIAAN M. KLAIJ<sup>§</sup>

5                   **Abstract.** The augmented Lagrangian (AL) preconditioner and its variants have been success-  
6 fully applied to solve saddle point systems arising from the incompressible Navier-Stokes equations  
7 discretized by the finite element method. Attractive features are the purely algebraic construction  
8 and robustness with respect to the Reynolds number and mesh refinement. In this paper, we recon-  
9 sider the application of the AL preconditioner in the context of the stabilized finite volume methods  
10 and present the extension to the Reynolds-Averaged Navier-Stokes (RANS) equations, which are  
11 used to model turbulent flows in industrial applications. Furthermore, we propose a new variant of  
12 the AL preconditioner, obtained by substituting the approximation of the Schur complement from  
13 the SIMPLE preconditioner into the inverse of the Schur complement for the AL preconditioner.  
14 This new variant is applied to both Navier-Stokes and RANS equations to compute laminar and  
15 turbulent boundary-layer flows on grids with large aspect ratios. Spectral analysis shows that the  
16 new variant yields a more clustered spectrum of eigenvalues away from zero, which explains why it  
17 outperforms the existing variants in terms of the number of the Krylov subspace iterations.

18                   **Key words.** Reynolds-Averaged Navier-Stokes equations, finite volume method, Block struc-  
19 tured preconditioner, augmented Lagrangian preconditioner, SIMPLE preconditioner.

20                   **AMS subject classifications.** 65F10, 65F08

21                   **1. Introduction.** The augmented Lagrangian (AL) preconditioner [2], belong-  
22 ing to the class of block structured preconditioners [9, 26, 27], is originally proposed  
23 to solve saddle point systems arising from the incompressible Navier-Stokes equations  
24 discretized by the finite element method (FEM). The AL preconditioner features a  
25 purely algebraic construction and robustness with respect to the Reynolds number  
26 and mesh refinement. Because of these attractive features, recent research was de-  
27 voted to the further development and extension of the AL preconditioner, notably the  
28 modified variants [3–5] with reduced computational complexity and the extension [32]  
29 to the context of stabilized finite volume methods (FVM), which are widely used in  
30 industrial computational fluid dynamic (CFD) applications.

31                   Although applying FEM and FVM to the incompressible Navier-Stokes equations  
32 both leads to saddle point systems, the extension from FEM to FVM is nontrivial, see  
33 [32] for a detailed discussion on the dimensionless parameter that is involved in the AL  
34 preconditioner, its influence on the convergence of both nonlinear and linear iterations  
35 and the proposed rule to choose the optimal value in practice. We observed that the  
36 features of the AL preconditioner exhibited in the FEM context, e.g. the robustness  
37 with respect to the Reynolds number and mesh refinement, are maintained in the  
38 context of FVM, at least for academic benchmarks. This motivates us to consider the  
39 application of the AL preconditioner in the broader context of Reynolds-Averaged  
40 Navier-Stokes (RANS) equations, which are used to model turbulent flows in industrial

---

\*Submitted to the editors DATE.

<sup>†</sup>State Key Laboratory of Computer Architecture, Institute of Computing Technology, Chinese Academy of Sciences, No.6 Kexueyuan South Road Zhongguancun Haidian District Beijing, P.R. China 100190. (hexin2016@ict.ac.cn, <http://english.ict.cas.cn/>).

<sup>‡</sup>Delft Institute of Applied Mathematics, Delft University of Technology, Mekelweg 4, 2628 CD Delft, The Netherlands. (c.vuik@tudelft.nl, <http://www.ewi.tudelft.nl/>).

<sup>§</sup>Maritime Research Institute Netherlands, P.O. Box 28, 6700 AA Wageningen, The Netherlands. (c.klaij@marin.nl, <http://www.marin.nl/>).

41 CFD applications. These equations are obtained by applying the Reynolds averaging  
 42 process to the Navier-Stokes equations and adding an eddy-viscosity turbulence model  
 43 to close the system, see [11,23,30]. Such models represent the effect of turbulence on  
 44 the averaged flow quantities through a locally increased viscosity.

45 Unfortunately, straightforward application of the AL preconditioner to the RANS  
 46 equations yields disappointing results as we will show in this paper. Therefore, we  
 47 reconsider the approximation of the Schur complement which is the key to the effi-  
 48 cient block structured preconditioners [1,24]. In [15], we compared the exact Schur  
 49 preconditioner with several cheaper approximations, including SIMPLE, for three test  
 50 cases from maritime engineering, characterized by the thin turbulent boundary layers  
 51 on grids with high aspect ratios. In this paper, we propose a new Schur complement  
 52 approximation which leads to a new variant of the AL preconditioner. The approach  
 53 is to substitute the approximation of the Schur complement from the SIMPLE precon-  
 54 ditioner [14,16] into the inverse of the Schur complement for the AL preconditioner.  
 55 This choice is motivated by the simplicity that in the utilised FVM the Schur comple-  
 56 ment approximation from the SIMPLE preconditioner reduces to a scaled Laplacian  
 57 matrix [14,16] and the efficiency of the SIMPLE preconditioner on the complicated  
 58 maritime applications [15,16]. As we will show, the new variant of the AL precondi-  
 59 tioner significantly speeds up the convergence rate of the Krylov subspace solvers for  
 60 both turbulent and laminar boundary-layer flows computed with a stabilized FVM.

61 The structure of this paper is as follows. The Reynolds-Averaged Navier-Stokes  
 62 equations and the discretization and solution methods are introduced in Section 2.  
 63 The new method to construct the approximation of the Schur complement in the AL  
 64 preconditioner is presented in Section 3, followed by a brief recall of the old approach.  
 65 A comparison with the SIMPLE preconditioner in Section 3.4 is based on a basic  
 66 cost model presented in Section 4. Section 5 includes the numerical experiments  
 67 carried out on the turbulent and laminar benchmarks. Conclusions and future work  
 68 are outlined in Section 6.

69 **2. Governing equations and solution techniques.** In this section, we in-  
 70 troduce the Reynolds-Averaged Navier-Stokes equations as well as the finite volume  
 71 discretization and solution methods.

72 **2.1. Reynolds-Averaged Navier-Stokes equations.** Incompressible, turbu-  
 73 lent flows often occur in the CFD applications of the maritime industry. Most com-  
 74 mercial and open-source CFD packages rely on the Reynolds-Averaged Navier-Stokes  
 75 (RANS) equations to model such flows [11,23,30] since more advanced models, such as  
 76 the Large-Eddy Simulation (LES), are still too expensive for industrial applications.  
 77 Besides, engineers are firstly interested in the averaged properties of a flow, such as  
 78 the average forces on a body, which is exactly what RANS models provide.

79 The RANS equations are obtained from the Navier-Stokes equations by an aver-  
 80 aging process referred to as the Reynolds averaging, where an instantaneous quantity  
 81 such as the velocity, is decomposed into its averaged and fluctuating part. If the flow  
 82 is statistically steady, time averaging is used and ensemble averaging is applied for  
 83 unsteady flows. The averaged part is solved for, while the fluctuating part is mod-  
 84 elled which requires additional equations, for instance for the turbulent kinetic energy  
 85 and turbulence dissipation, see [11,23,30] for a broader discussion. The Reynolds-  
 86 Averaged momentum and continuity equations are here presented in the conservative

87 form using FVM for a control volume  $\Omega$  with surface  $S$  and outward normal vector  $\mathbf{n}$ :

$$88 \quad (1) \quad \int_S \rho \mathbf{u} \mathbf{u} \cdot \mathbf{n} dS + \int_S P \mathbf{n} dS - \int_S \mu_{\text{eff}} (\nabla \mathbf{u} + \nabla \mathbf{u}^T) \cdot \mathbf{n} dS = \int_{\Omega} \rho \mathbf{b} d\Omega,$$

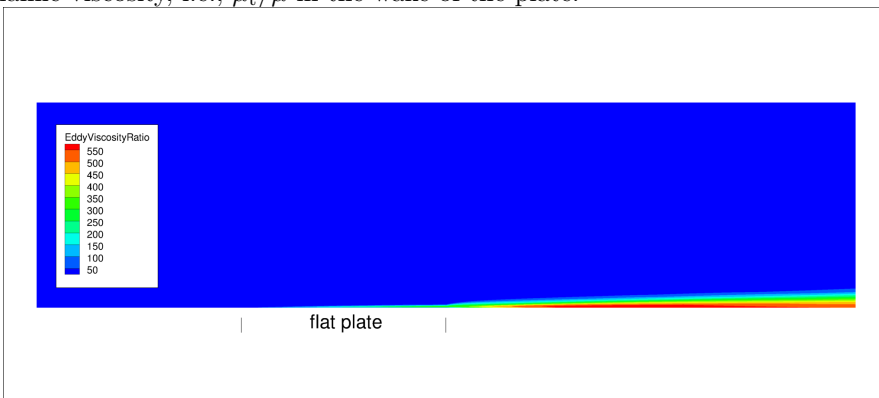
$$\int_S \mathbf{u} \cdot \mathbf{n} dS = 0$$

89 where  $\mathbf{u}$  is the velocity,  $P = p + \frac{2}{3} \rho k$  consists of the pressure  $p$  and the turbulent kinetic  
 90 energy  $k$ ,  $\rho$  is the (constant) density,  $\mu_{\text{eff}}$  is the (variable) effective viscosity and  $\mathbf{b}$  is a  
 91 given force field. On the boundaries we either impose the velocity ( $\mathbf{u} = \mathbf{u}_{\text{ref}}$  on inflow  
 92 and  $\mathbf{u} = 0$  on walls) or the normal stress ( $\mu_{\text{eff}} \frac{\partial \mathbf{u}}{\partial \mathbf{n}} - P \mathbf{n} = 0$  on outflow and farfield).  
 93 The effective viscosity  $\mu_{\text{eff}}$  is the sum of the constant dynamic viscosity  $\mu$  and the  
 94 variable turbulent eddy viscosity  $\mu_t$  provided by the turbulence model as a function  
 95 of  $k$  and possibly of other turbulence quantities. Notice that for laminar flows, where  
 96  $k$  and  $\mu_t$  are zero, the RANS equations reduce to the Navier-Stokes equations.

97 In this paper, we will consider laminar flow of water over a finite flat plate at  
 98  $\text{Re} = 10^5$  and turbulent flow at  $\text{Re} = 10^7$ . The density and dynamic viscosity of  
 99 water at atmospheric pressure and 20 degrees Celsius are roughly  $\rho = 1000[\text{kg}/\text{m}^3]$   
 100 and  $\mu = 0.001[\text{kg}/\text{m}/\text{s}]$ , see [31]. The inflow velocity  $\mathbf{u}_{\text{ref}}$  in  $[\text{m}/\text{s}]$  is adjusted to  
 101 obtain the given Reynolds number  $\text{Re} = \frac{\rho \|\mathbf{u}_{\text{ref}}\| L_{\text{ref}}}{\mu}$  based on the length  $L_{\text{ref}} = 1[\text{m}]$   
 102 of the plate. The flow is characterized by a very thin boundary layer on the plate  
 103 which is fully resolved by stretching the grid in the vertical direction. This inevitably  
 104 results in high aspect-ratio cells near the plate. At the higher Reynolds number, the  
 105 flow becomes turbulent in this thin boundary layer and in the wake of the plate.  
 106 Figure 1 illustrates how the effective viscosity (provided in this case by the  $k$ - $\omega$  SST  
 107 model [20]) varies in the domain: the eddy viscosity in the wake of the plate is two  
 108 orders of magnitude larger than the dynamic viscosity. We will also consider turbulent  
 109 flow over a backward-facing step at Reynolds  $5 \cdot 10^4$  based on the step height, which  
 110 has similar eddy-viscosity magnitude in the wake of the step.

111 Solvers for the RANS equations should be able to handle both challenges, i.e.  
 112 high-aspect ratio cells and significant variation in viscosity.

Fig. 1: For the turbulent flat plate problem, the ratio between the eddy viscosity and dynamic viscosity, i.e.,  $\mu_t/\mu$  in the wake of the plate.



113 **2.2. Linear saddle point system.** As explained in [15], the nonlinear system  
 114 (1) is solved for  $\mathbf{u}$  and  $P$  as a series of linear systems obtained by Picard linearization  
 115 [11], i.e. by assuming that the mass flux  $\rho \mathbf{u} \cdot \mathbf{n}$ , the turbulent kinetic energy  $k$  and

116 the effective viscosity  $\mu_{\text{eff}}$  are known from the previous iteration. The turbulence  
 117 equations are then solved for  $k$  and possibly other turbulence quantities, after which  
 118 the process is repeated until a convergence criterion is met.

119 After linearization and discretization of system (1) by the cell-centered and co-  
 120 located FVM [11], the linear system is in saddle point form as

$$121 \quad (2) \quad \begin{bmatrix} Q & G \\ D & C \end{bmatrix} \begin{bmatrix} \mathbf{u} \\ p \end{bmatrix} = \begin{bmatrix} \mathbf{f} \\ g \end{bmatrix} \quad \text{with} \quad \mathcal{A} := \begin{bmatrix} Q & G \\ D & C \end{bmatrix},$$

122 where  $Q$  corresponds to the convection-diffusion operator and the matrices  $G$  and  $D$   
 123 denote the gradient and divergence operators, respectively. The matrix  $C$  comes from  
 124 the stabilization method. The details of these matrices are presented as follows.

125 The linearization and the explicit treatment of the second diffusion term  $\mu_{\text{eff}} \nabla \mathbf{u}^T \cdot$   
 126  $\mathbf{n}$  by using the velocity and effective viscosity from the previous iteration make the  
 127 matrix  $Q$  of a block diagonal form. Each diagonal part  $Q_{ii}$  is equal and contains  
 128 the contributions from the convective term  $\rho u_i \mathbf{u} \cdot \mathbf{n}$  and the remaining diffusion term  
 129  $\mu_{\text{eff}} \nabla u_i \cdot \mathbf{n}$ .

130 In FEM the divergence matrix is the negative transpose of the gradient matrix,  
 131 i.e.  $D = -G^T$ . However, in FVM we have  $D_i = G_i$  on structured and unstructured  
 132 grids, where  $i$  denotes the components therein. Only for structured grids we have  
 133 that  $D$  is skew-symmetric ( $D_i = -D_i^T$ ) and therefore that  $D = -G^T$  as in FEM. We  
 134 refer to [11] for the details of  $D$  and  $G$  in FVM.

135 To avoid pressure oscillations when the velocity and pressure are co-located in the  
 136 cell centers, the pressure-weighted interpolation (PWI) method [21] is applied here  
 137 and leads to the stabilization matrix  $C$  as

$$138 \quad (3) \quad C = D \text{diag}^{-1}(Q)G - \text{diag}^{-1}(Q_{ii})L_p,$$

139 where  $L_p$  is the Laplacian matrix. The details about the PWI method and its repre-  
 140 sentation by the discrete matrices as (3) are given in [14, 16].

141 **2.3. Preconditioners for saddle point systems.** Block structured precondition-  
 142 ers are used to accelerate the convergence rate of the Krylov subspace solvers for  
 143 saddle point systems as (2). They are based on the block  $\mathcal{LDU}$  decomposition of the  
 144 coefficient matrix given by

$$145 \quad (4) \quad \mathcal{A} = \mathcal{LDU} = \begin{bmatrix} Q & G \\ D & C \end{bmatrix} = \begin{bmatrix} I & O \\ DQ^{-1} & I \end{bmatrix} \begin{bmatrix} Q & O \\ O & S \end{bmatrix} \begin{bmatrix} I & Q^{-1}G \\ O & I \end{bmatrix},$$

146 where  $S = C - DQ^{-1}G$  is the so-called Schur complement. To successfully design  
 147 block structured preconditioners, a combination of this block factorization with a suit-  
 148 able approximation of the Schur complement is utilized. It is not practical to explicitly  
 149 form the exact Schur complement due to the action of  $Q^{-1}$  typically when the size is  
 150 large. This implies that constructing the spectrally equivalent and numerically cheap  
 151 approximations of the Schur complement can be very challenging. There exist several  
 152 state-of-the-art approximations of the Schur complement, e.g. the least-square com-  
 153 mutator (LSC) [8], pressure convection-diffusion (PCD) operator [13, 28], SIMPLE(R)  
 154 preconditioner [16, 17, 29], and augmented Lagrangian (AL) approach [2-4, 32] etc.  
 155 These Schur complement approximations are originally designed in the context of  
 156 stable FEM where the (2, 2) block of  $\mathcal{A}$  is zero. We refer for more details of the Schur  
 157 approximation to the surveys [1, 24, 26, 27] and the books [9, 22].

158 This paper is meant to significantly improve the efficiency of the AL preconditioner in the turbulent and laminar boundary-layer flows computed with a stabilized  
 159 FVM. To fulfil the objective of this paper, a new variant of the AL preconditioner  
 160 is proposed, which substitutes the approximation of the Schur complement from the  
 161 SIMPLE preconditioner into the inverse of the Schur complement for the AL preconditioner. More details are presented in the next section.  
 162  
 163

164 **3. Augmented Lagrangian preconditioner.** In this section, we propose the  
 165 new method to construct the approximation of the Schur complement in the AL  
 166 preconditioner, followed by the comparison with the old approach.

167 **3.1. Transformation of the linear system.** It is observed in [2,3] that applying  
 168 the AL preconditioner allows us to circumvent the challenging issue of constructing  
 169 the numerically cheap and spectrally equivalent approximation of the Schur complement  $S$  of the original system (2). To apply the AL preconditioner, the original system  
 170 (2) is transformed into an equivalent one with the same solution [3,32], which is of  
 171 the form  
 172

$$173 \quad (5) \quad \begin{bmatrix} Q_\gamma & G_\gamma \\ D & C \end{bmatrix} \begin{bmatrix} \mathbf{u} \\ p \end{bmatrix} = \begin{bmatrix} \mathbf{f}_\gamma \\ g \end{bmatrix} \quad \text{with} \quad \mathcal{A}_\gamma := \begin{bmatrix} Q_\gamma & G_\gamma \\ D & C \end{bmatrix},$$

174 where  $Q_\gamma = Q - \gamma GW^{-1}D$ ,  $G_\gamma = G - \gamma GW^{-1}C$  and  $\mathbf{f}_\gamma = \mathbf{f} - \gamma GW^{-1}g$ . The scalar  
 175  $\gamma > 0$  and the matrix  $W$  should be non-singular. This transformation is obtained by  
 176 multiplying  $-\gamma GW^{-1}$  on both sides of the second row of system (2) and adding the  
 177 resulting equation to the first one. Clearly, the transformed system (5) has the same  
 178 solution as system (2) for any value of  $\gamma$  and any non-singular matrix  $W$ . The Schur  
 179 complement of  $\mathcal{A}_\gamma$  is  $S_\gamma = C - DQ_\gamma^{-1}G_\gamma$ .

180 The equivalent system (5) is what we want to solve when applying the AL preconditioner.  
 181 Using the block  $\mathcal{DU}$  decomposition of  $\mathcal{A}_\gamma$ , the ideal AL preconditioner  
 182  $\mathcal{P}_{IAL}$  is given by

$$183 \quad (6) \quad \mathcal{P}_{IAL} = \begin{bmatrix} Q_\gamma & G_\gamma \\ O & \tilde{S}_\gamma \end{bmatrix},$$

184 where  $\tilde{S}_\gamma$  denotes the approximation of  $S_\gamma$ .

185 The modified variant of the ideal AL preconditioner, i.e., the so-called modified  
 186 AL preconditioner, replaces  $Q_\gamma$  by its block lower-triangular part, i.e.  $\tilde{Q}_\gamma$ , such that  
 187 the difficulty of solving sub-systems with  $Q_\gamma$  is avoided [3]. To see it more clearly, we  
 188 take a 2D case as an example and give  $Q_\gamma$  and  $\tilde{Q}_\gamma$  as follows

$$189 \quad Q = \begin{bmatrix} Q_1 & O \\ O & Q_1 \end{bmatrix}, G = \begin{bmatrix} G_1 \\ G_2 \end{bmatrix}, D = [D_1 \quad D_2],$$

$$190$$

$$191 \quad Q_\gamma = \begin{bmatrix} Q_1 - \gamma G_1 W^{-1} D_1 & -\gamma G_1 W^{-1} D_2 \\ -\gamma G_2 W^{-1} D_1 & Q_1 - \gamma G_2 W^{-1} D_2 \end{bmatrix},$$

$$192$$

$$193 \quad \tilde{Q}_\gamma = \begin{bmatrix} Q_1 - \gamma G_1 W^{-1} D_1 & O \\ -\gamma G_2 W^{-1} D_1 & Q_1 - \gamma G_2 W^{-1} D_2 \end{bmatrix}.$$

194 Substituting  $\tilde{Q}_\gamma$  into  $\mathcal{P}_{IAL}$  as (6), then we get the modified AL preconditioner  $\mathcal{P}_{MAL}$ :

$$195 \quad (7) \quad \mathcal{P}_{MAL} = \begin{bmatrix} \tilde{Q}_\gamma & G_\gamma \\ O & \tilde{S}_\gamma \end{bmatrix}.$$

196 It appears that one needs to solve sub-systems with  $\tilde{Q}_\gamma$  when applying  $\mathcal{P}_{MAL}$ .  
 197 This work is further reduced to solve systems with  $Q_1 - \gamma G_1 W^{-1} D_1$  and  $Q_1 -$   
 198  $\gamma G_2 W^{-1} D_2$ . These two sub-blocks do not contain the coupling between two com-  
 199 ponents of the velocity so that it is much easier to solve, compared to  $Q_\gamma$  involved in  
 200  $\mathcal{P}_{IAL}$ .

201 **3.2. New Schur complement approximation.** The key of the ideal and mod-  
 202 ified AL preconditioners is to find a numerically cheap and spectrally equivalent Schur  
 203 complement approximation  $\tilde{S}_\gamma$ . The novel approximation proposed by this paper is  
 204 based on the following lemma.

205 **LEMMA 3.1.** *Assuming that all the relevant matrices are invertible, then the in-*  
 206 *verse of  $S_\gamma$  is given by*

$$207 \quad (8) \quad S_\gamma^{-1} = S^{-1}(I - \gamma C W^{-1}) + \gamma W^{-1},$$

208 where  $S = C - DQ^{-1}G$  denotes the Schur complement of the original system (2).

209 Proof. We refer to [3, 32] for the proof. ■

210 This lemma was already published but its importance was not fully appreciated.  
 211 Since Lemma 3.1 gives the connection between the Schur complement  $S_\gamma$  and  $S$ , it  
 212 provides a framework to build the approximation of  $S_\gamma$ . Provided an approximation  
 213 of  $S$  denoted by  $\tilde{S}$ , it is natural to substitute  $\tilde{S}$  into expression (8) to construct an  
 214 approximation of  $S_\gamma$  in the inverse form as

$$215 \quad (9) \quad \tilde{S}_{\gamma \text{ new}}^{-1} = \tilde{S}^{-1}(I - \gamma C W^{-1}) + \gamma W^{-1},$$

216 where the notation *new* is used to differ from the old approach to approximate  $S_\gamma$ ,  
 217 discussed in the next section.

218 Actually it is not necessary to explicitly implement  $\tilde{S}_{\gamma \text{ new}}$ . Solving a sub-system  
 219 with  $\tilde{S}_{\gamma \text{ new}}$ , i.e.,  $\tilde{S}_{\gamma \text{ new}} \mathbf{x} = \mathbf{b}$ , converts to multiply the vector  $\mathbf{b}$  on both sides of  
 220 expression (9). Supposed that  $W$  is a diagonal matrix, e.g. the mass matrix  $M_p$  with  
 221 density multiplied with cell volumes in FVM, the complexity of  $(\tilde{S}^{-1}(I - \gamma C W^{-1}) +$   
 222  $\gamma W^{-1})\mathbf{b}$  is focused on solving the system with  $\tilde{S}$ . This means that the accelerating  
 223 techniques to optimize  $\tilde{S}$  can reduce the computational time of the new approach.

224 From expression (9) it is clear that the Schur complement approximation  $\tilde{S}$  pro-  
 225 posed for the original system (2) is used to construct  $\tilde{S}_{\gamma \text{ new}}$  here. Among the known  
 226 LSC, PCD and SIMPLE methods, this paper chooses the Schur complement approx-  
 227 imation arising from the SIMPLE preconditioner. One motivation is that in the  
 228 context of the considered FVM the Schur complement approximation from the SIM-  
 229 PLE preconditioner reduces to a scaled Laplacian matrix. See more details in the next  
 230 paragraph. This choice is also motivated by the efficiency of the SIMPLE precondi-  
 231 tioner on the complicated maritime applications, see [15, 16] for instance. We expect  
 232 that the choice of the Schur complement approximation arising from the SIMPLE  
 233 preconditioner helps to build a numerically cheap and efficient  $\tilde{S}_{\gamma \text{ new}}$ .

234 Regarding the Schur complement  $S = C - DQ^{-1}G$  of the original system (2), the  
 235 SIMPLE preconditioner approximates  $Q$  by its diagonal,  $\text{diag}(Q)$ , and obtains the  
 236 approximation of  $S$  as  $\tilde{S}_1 = C - D\text{diag}^{-1}(Q)G$ . Taking into account the stabilization  
 237 matrix  $C = D\text{diag}^{-1}(Q)G - \text{diag}^{-1}(Q_{ii})L_p$  as given in (3), we further reduce the  
 238 approximation to  $\tilde{S}_{\text{SIMPLE}} = -\text{diag}^{-1}(Q_{ii})L_p$  because the term  $D\text{diag}^{-1}(Q)G$  in  $\tilde{S}_1$   
 239 and  $C$  cancels. See, for instance, [14, 16] for a detailed discussion of obtaining  $\tilde{S}_{\text{SIMPLE}}$

240 in FVM. Substituting  $\tilde{S}_{\text{SIMPLE}}$  and  $W = M_p$  into expression (9) we obtain

241 (10)  $\tilde{S}_{\gamma_{\text{new}}}^{-1} = \tilde{S}_{\text{SIMPLE}}^{-1}(I - \gamma C M_p^{-1}) + \gamma M_p^{-1}$ , where  $\tilde{S}_{\text{SIMPLE}} = -\text{diag}^{-1}(Q_{ii})L_p$ .

242 Based on the above approach, it is seen that there is no extra requirement on  
 243 the value of the parameter  $\gamma$  so that  $\tilde{S}_{\gamma_{\text{new}}}$  can be obtained. As pointed out in the  
 244 next section, the requirements in the old approximation of the Schur complement  
 245 are contradictory. This suggests that the convergence rate of the Krylov subspace  
 246 solvers preconditioned by the AL preconditioner with the new Schur complement  
 247 approximation is weakly depending on the value of  $\gamma$ . This advantage makes the new  
 248 AL variant less sensitive to the choice of  $\gamma$ . See the results regarding the influence of  
 249  $\gamma$  on the convergence rate in the numerical experiment section.

250 **3.3. Old Schur complement approximation.** For a comparison reason, the  
 251 old approximation of the Schur complement in the AL preconditioner is recalled in  
 252 this section. The starting point to construct the old approximation of the Schur  
 253 complement in the AL preconditioner is also Lemma 3.1. However, the strategy is  
 254 totally different. Choosing  $W_1 = \gamma C + M_p$  and substituting  $W_1$  into expression (8)  
 255 we have

256 
$$\begin{aligned} S_{\gamma}^{-1} &= S^{-1}(I - (\gamma C + M_p - M_p)(\gamma C + M_p)^{-1}) + \gamma(\gamma C + M_p)^{-1} \\ &= S^{-1}M_p(\gamma C + M_p)^{-1} + \gamma(\gamma C + M_p)^{-1} \\ &= (\gamma^{-1}S^{-1}M_p + I)(C + \gamma^{-1}M_p)^{-1}. \end{aligned}$$

257 For large values of  $\gamma$  such that  $\|\gamma^{-1}S^{-1}M_p\| \ll 1$ , the term  $\gamma^{-1}S^{-1}M_p$  can be  
 258 neglected so that we have  $\tilde{S}_{\gamma_{\text{old}}}$  as follows

259 (11) 
$$\tilde{S}_{\gamma_{\text{old}}} = C + \gamma^{-1}M_p.$$

260 The choice of  $W_1 = \gamma C + M_p$  is not practical since the action of  $W_1^{-1}$  is needed  
 261 in the transformed system (5). The ideal and modified AL preconditioners, used for  
 262 instance in [3,32], omit the term  $\gamma C$  in  $W_1$  and choose  $W = M_p$ . The choice  $W = M_p$   
 263 only involves the mass matrix  $M_p$ , which is easily inverted especially in FVM where  
 264  $M_p$  is a diagonal matrix.

265 The contradictory requirements in the above method are presented as follows.  
 266 The approximation  $\tilde{S}_{\gamma_{\text{old}}}$  is obtained if and only if  $W_1 = \gamma C + M_p$  and large values  
 267 of  $\gamma$  are chosen. However,  $W = M_p$  is close to  $W_1 = \gamma C + M_p$  only when  $\gamma$  is  
 268 small. This means that it is contradictory to tune the value of  $\gamma$  so that  $W = M_p$   
 269 and  $\tilde{S}_{\gamma_{\text{old}}}$  could be simultaneously obtained. A simply balanced value of  $\gamma$  is  $\gamma = 1$   
 270 or  $O(1)$ . This disadvantage reflects in the convergence rate of the Krylov subspace  
 271 solvers. This paper shows that for the laminar calculations the number of the Krylov  
 272 subspace iterations preconditioned by the AL preconditioner with  $\tilde{S}_{\gamma_{\text{old}}}$  is about  
 273 fourteen times larger than the new Schur approximation  $\tilde{S}_{\gamma_{\text{new}}}$ . An application of  
 274 the AL preconditioner with  $\tilde{S}_{\gamma_{\text{old}}}$  in the more challenging turbulent computations  
 275 with variable viscosity and more stretched grids shows a very slow convergence or  
 276 even stagnation. See numerical experiments in Section 5.

277 In summary, regarding the ideal and modified AL preconditioners applied to the  
 278 transformed system (5), there are two types of Schur complement approximations, i.e.

- 279 1.  $\tilde{S}_{\gamma_{\text{new}}}^{-1} = \tilde{S}_{\text{SIMPLE}}^{-1}(I - \gamma C M_p^{-1}) + \gamma M_p^{-1}$ ,  $\tilde{S}_{\text{SIMPLE}} = -\text{diag}^{-1}(Q_{ii})L_p$ .  
 280 2.  $\tilde{S}_{\gamma_{\text{old}}} = C + \gamma^{-1}M_p$ .

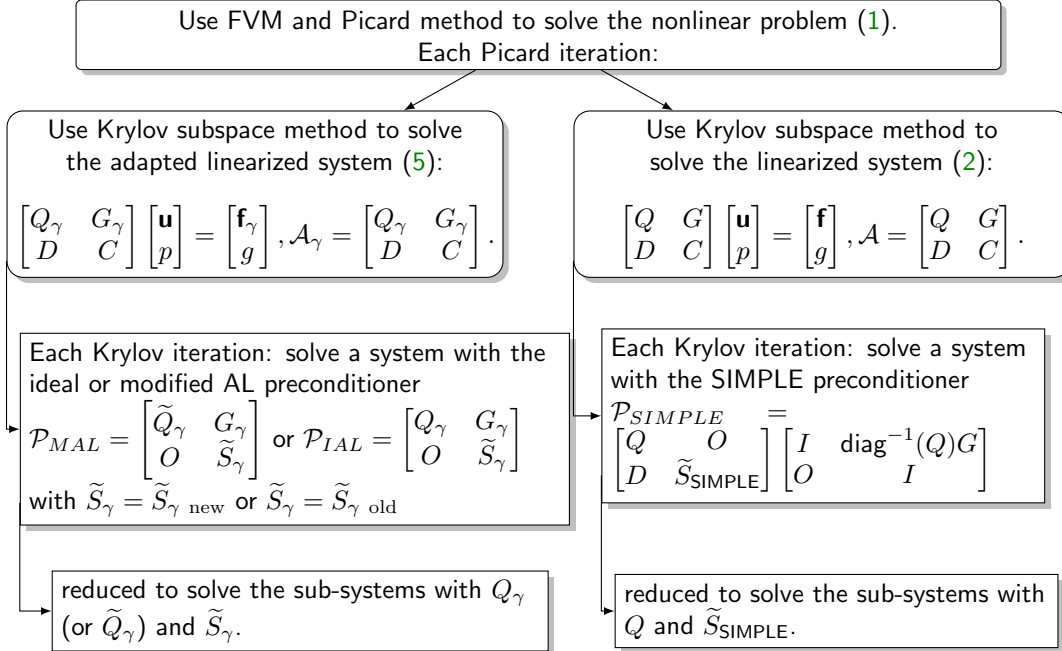
281 The choice of  $W = M_p$  is fixed in the transformation to obtain the equivalent system  
 282 (5) and the construction of two Schur complement approximations.

283 **3.4. SIMPLE preconditioner.** Although the focus of this paper is on the  
 284 new Schur complement approximation and its advantage over the old one in the AL  
 285 preconditioner, we also present the SIMPLE preconditioner for a more comprehensive  
 286 comparison. Different from the ideal AL preconditioner and its modified variant, the  
 287 SIMPLE preconditioner is proposed for the original system (2), which is based on the  
 288 block  $\mathcal{LDU}$  decomposition of the coefficient matrix  $\mathcal{A}$  and given by

$$289 \quad \mathcal{P}_{SIMPLE} = \begin{bmatrix} Q & O \\ D & \tilde{S} \end{bmatrix} \begin{bmatrix} I & \text{diag}^{-1}(Q)G \\ O & I \end{bmatrix},$$

290 where  $\tilde{S}$  denotes the approximation of the Schur complement of  $\mathcal{A}$ , i.e.,  $S = C -$   
 291  $DQ^{-1}G$ . With the stabilization matrix  $C$  given by (3), the Schur complement ap-  
 292 proximation becomes  $\tilde{S} = \tilde{S}_{SIMPLE} = -\text{diag}^{-1}(Q_{ii})L_p$  where  $L_p$  is the Laplacian  
 293 matrix. Therefore, the scaled Laplacian matrix is used as the approximation of the  
 294 Schur complement in the SIMPLE preconditioner. In order to avoid repetition we  
 295 refer to Section 3.2 for the details of obtaining  $\tilde{S}_{SIMPLE}$ . We refer to [15, 16] for the  
 296 performance of the SIMPLE preconditioner in the FVM context on both academic  
 297 and maritime applications.

298 **4. Cost model for AL and SIMPLE preconditioners.** To summarize the  
 299 linearized systems where the AL and SIMPLE preconditioners are applied individu-  
 300 ally, we give the schematic diagram as follows:  
 301



302 In [15], we presented a basic cost model to distinguish between the SIMPLE pre-  
 303 preconditioner and other preconditioners. Here, we extend the model to include the  
 304 modified AL preconditioner with two Schur complement approximations. Firstly con-  
 305 sider the cost of using the SIMPLE preconditioner  $\mathcal{P}_{SIMPLE}$  for a Krylov subspace  
 306 method that solves the system with  $\mathcal{A}$  to a certain relative tolerance in  $n_1$  iterations.  
 307 The preconditioner is applied at each Krylov iteration and the SIMPLE precondi-  
 308 tioner solves the momentum sub-system 'mom-u' with  $Q$  and the pressure sub-system  
 309

310 'mass-p' with  $\tilde{S}_{\text{SIMPLE}}$ . Besides, at each Krylov iteration another cost is expressed in  
 311 the product of the coefficient matrix  $\mathcal{A}$  with a Krylov residual vector  $\mathbf{b}_{res}$ . Thus, the  
 312 total cost is

313 •  $\mathcal{P}_{\text{SIMPLE}}$ :  $n_1 \times (\text{mom-u with } Q + \text{mass-p with } \tilde{S}_{\text{SIMPLE}} + \mathcal{A} \times \mathbf{b}_{res})$ .

314 Secondly consider the cost of applying the modified AL preconditioner  $\mathcal{P}_{\text{MAL}}$   
 315 with the new Schur approximation  $\tilde{S}_{\gamma \text{ new}}$ . If we neglect the multiplications in the  
 316 definition of  $\tilde{S}_{\gamma \text{ new}}$  as given in (10), the cost of solving the pressure sub-system with  
 317  $\tilde{S}_{\gamma \text{ new}}$  is the same as  $\tilde{S}_{\text{SIMPLE}}$ . Thus, the total cost is

318 •  $\mathcal{P}_{\text{MAL}}$  with  $\tilde{S}_{\gamma \text{ new}}$ :  $n_2 \times (\text{mom-u with } \tilde{Q}_{\gamma} + \text{mass-p with } \tilde{S}_{\text{SIMPLE}} + \mathcal{A}_{\gamma} \times \mathbf{b}_{res})$ .

319 Finally consider the cost of applying the modified AL preconditioner  $\mathcal{P}_{\text{MAL}}$  with  
 320 the old Schur approximation  $\tilde{S}_{\gamma \text{ old}}$ . Similar to the analysis of  $\mathcal{P}_{\text{MAL}}$  with  $\tilde{S}_{\gamma \text{ new}}$ , we  
 321 obtain the total cost as

322 •  $\mathcal{P}_{\text{MAL}}$  with  $\tilde{S}_{\gamma \text{ old}}$ :  $n_3 \times (\text{mom-u with } \tilde{Q}_{\gamma} + \text{mass-p with } \tilde{S}_{\gamma \text{ old}} + \mathcal{A}_{\gamma} \times \mathbf{b}_{res})$ .

323 Clearly, the difference of cost by applying  $\mathcal{P}_{\text{MAL}}$  with  $\tilde{S}_{\gamma \text{ new}}$  and  $\tilde{S}_{\gamma \text{ old}}$  arises from  
 324 solving the pressure sub-systems with  $\tilde{S}_{\text{SIMPLE}}$  and  $\tilde{S}_{\gamma \text{ old}}$ , respectively. It is difficult  
 325 to analytically compare the complexity of solving the sub-systems with  $\tilde{S}_{\text{SIMPLE}}$  and  
 326  $\tilde{S}_{\gamma \text{ old}}$ . However, numerical experiments in the next section show  $n_2 \ll n_3$  on all  
 327 considered problems, which makes the new Schur complement approximation more  
 328 efficient and attractive in terms of iterations and wall-clock time.

329 At each Krylov iteration, more nonzero fill-in introduced in the blocks  $Q_{\gamma}$  and  $G_{\gamma}$   
 330 and more difficulty of iteratively solving the momentum sub-system with  $\tilde{Q}_{\gamma}$  than  $Q$   
 331 lead to a higher cost of applying  $\mathcal{P}_{\text{MAL}}$  with  $\tilde{S}_{\gamma \text{ new}}$  than  $\mathcal{P}_{\text{SIMPLE}}$ . We refer to [32]  
 332 for a detailed discussion. Therefore, this higher cost of  $\mathcal{P}_{\text{MAL}}$  with  $\tilde{S}_{\gamma \text{ new}}$  only pays-  
 333 off if  $n_2 < n_1$ . In this paper we observe  $n_2 < n_1$  on the turbulent and laminar tests  
 334 but the time advantage of  $\mathcal{P}_{\text{MAL}}$  with  $\tilde{S}_{\gamma \text{ new}}$  over  $\mathcal{P}_{\text{SIMPLE}}$  needs further assessment  
 335 which is included in the future research plan.

336 **5. Numerical experiments.** In this section, we compare the new AL variant  
 337 with the old one and with SIMPLE preconditioner, for incompressible, laminar flow  
 338 governed by the Navier-Stokes equations, as well as turbulent flow governed by the  
 339 Reynolds-Averaged Navier-Stokes equations.

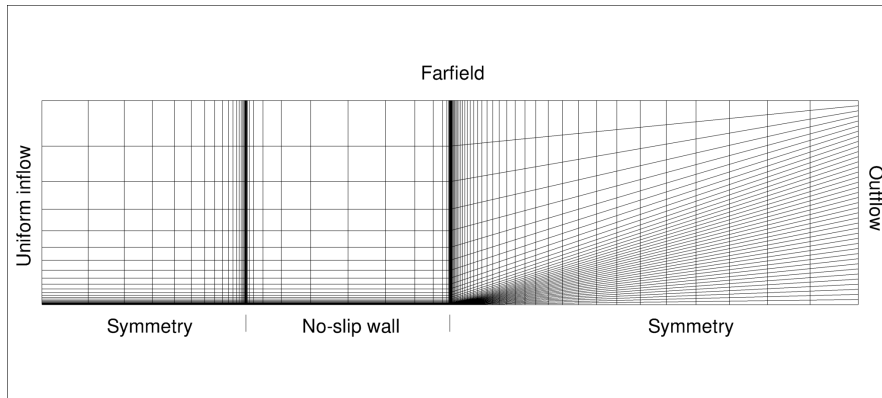
340 **5.1. Flow over a finite flat plate (FP).** Flow over a finite flat plate is a  
 341 standard test case in maritime engineering, see [25] for a detailed study of various  
 342 turbulence models with MARIN's CFD software package ReFRESH [19].

343 We first consider the fully turbulent flow at  $\text{Re} = 10^7$  on the block-structured  
 344 grids. The grids are refined near the leading and trailing edge of the plate and spread  
 345 out in the wake of the plate, see Figure 2(a), which leads to some eccentricity and  
 346 non-orthogonality. As can be seen, the grids are stretched in both the horizontal  
 347 and vertical direction and reach the maximal aspect ratio of order  $1 : 10^4$  near the  
 348 middle of the plate. The complete flow is computed, starting from uniform laminar  
 349 flow upstream of the plate.

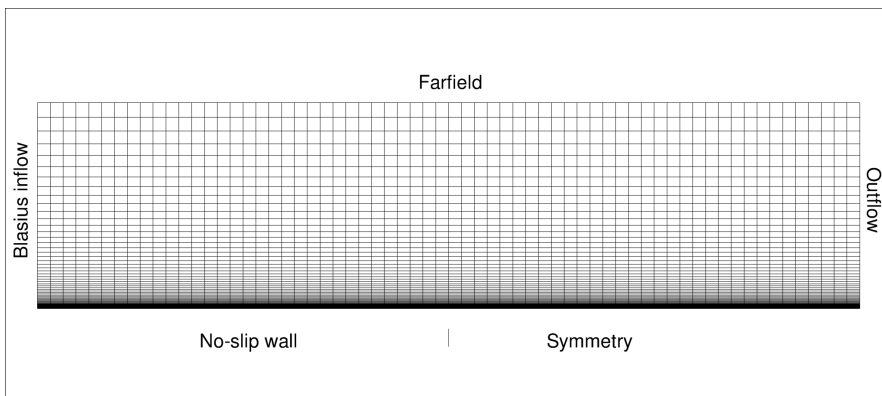
350 Second, we reconsider laminar flow at  $\text{Re} = 10^5$  on a straight single-block grid.  
 351 This case was already presented in [14–16, 32] for other solvers and preconditioners.  
 352 We reconsider it here to show that the new Schur complement approximation also  
 353 improves the efficiency of the AL preconditioner in the calculations of laminar flow.  
 354 The stretched grids shown in Figure 2(b) are generated based on uniform Cartesian  
 355 grids by applying the stretching function from [16] in the vertical direction. Near the  
 356 plate the grids have a maximal aspect ratio of order  $1 : 50$ , which is about two orders  
 357 smaller than the turbulent grids. Contrary to the turbulent case, the flow starts with

358 the (semi-analytical) Blasius solution halfway the plate, so only the second half and  
 359 the wake are computed.

Fig. 2: Impression of the grids. Turbulent case with  $80 \times 40$  cells and the max aspect ratio of order  $1 : 10^4$  and laminar case with  $64 \times 64$  cells and the max aspect ratio of order  $1 : 50$ .



(a) Turbulent case

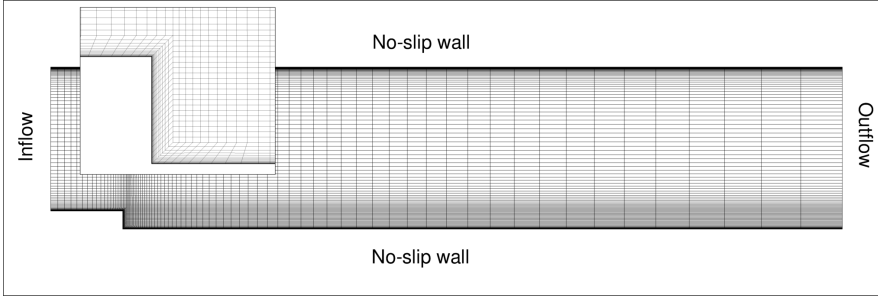


(b) Laminar case

360 **5.2. Flow over a backward-facing step (BFS).** We consider turbulent flow  
 361 over a backward-facing step in a channel, as measured by Driver and Seegmiller [6].  
 362 The chosen case corresponds to the C-30 case from the ERCOFTAC Classic Collec-  
 363 tion [10], with Reynolds number of  $5 \cdot 10^4$  based on the inflow velocity and the step  
 364 height. The flow is more complicated than the flat-plate flows as it features separa-  
 365 tion, a free shear-layer and reattachment. Detailed results with ReFRESKO for  
 366 various turbulence models are found in [7], including results for the  $k-\omega$  SST turbu-  
 367 lence model [20] used here. The grid is also more complicated: multiple blocks are  
 368 used to wrap the boundary layer around the step, see Figure 3.

369 In this paper all experiments are carried out based on the blocks  $Q$ ,  $G$ ,  $D$ ,  $C$ ,  $M_p$   
 370 and  $L_p$  and the right hand-side vector  $rhs$ , which are obtained at the 30th nonlinear  
 371 iteration. Numerical experiments in [32] show that the number of linear iterations  
 372 varies through the whole nonlinear procedure. The motivation of choosing the 30th  
 373 nonlinear iteration to export the blocks is that a representative number of linear  
 374 iteration can be obtained from the 30th nonlinear step, compared with the average

Fig. 3: Impression of block-structured grid with 9600 cells for turbulent flow over backward-facing step.



375 number of linear iterations through the whole nonlinear procedure. We use a series  
 376 of structured grids with  $80 \times 40$  and  $160 \times 80$  cells for the turbulent FP case and the  
 377 structured grid with 9600 cells for the turbulent BFS case. Regarding the laminar  
 378 FP calculation, we use a structured grid with  $64 \times 64$  cells. The matrices and right-  
 379 hand side vector are generated by ReFRESH and available in Matlab's binary .mat  
 380 format on the website [18]. The aim of the numerical experiments is to show the  
 381 variation in the eigenvalues and number of the Krylov subspace iterations, arising  
 382 from different Schur complement approximations in the AL preconditioner. To carry  
 383 out a comprehensive evaluation of the new Schur complement approximation in the  
 384 AL preconditioner, in this paper we solve the linear system preconditioned by the  
 385 AL preconditioner with the new Schur complement approximation to the machine  
 386 accuracy. For a fair comparison, the same stopping tolerance is used when employing  
 387 the old Schur complement approximation and the SIMPLE preconditioner. Since the  
 388 AL preconditioner with different Schur complement approximations and the SIMPLE  
 389 preconditioner involve various momentum or pressure sub-systems, all the sub-systems  
 390 are directly solved in this paper to avoid the sensitiveness of iterative solvers on the  
 391 varying solution complexities.

392 **5.3. Numerical experiments on the turbulent FP case.** To find out the  
 393 reason that the new Schur complement approximation  $\tilde{S}_{\gamma \text{ new}}$  leads to a fast conver-  
 394 gence of the Krylov subspace solvers preconditioned by the AL preconditioner, we plot  
 395 ten extreme eigenvalues of the preconditioned matrices  $\mathcal{P}_{IAL}^{-1}\mathcal{A}_{\gamma}$  and  $\mathcal{P}_{MAL}^{-1}\mathcal{A}_{\gamma}$  with  
 396  $\tilde{S}_{\gamma \text{ new}}$  on the grid with  $80 \times 40$  cells. The results which are shown in Figures 4 and  
 397 5 show that for the considered values of  $\gamma$  the smallest eigenvalues are far away from  
 398 zero and the spectrum is clustered due to a small ratio between the largest and small-  
 399 est magnitude of the eigenvalues. Such a distribution of the eigenvalues is favorable  
 400 for the Krylov subspace solvers and a fast convergence rate can be expected.

401 Results in Figure 6 show the fast convergence rate of the Krylov subspace solver  
 402 preconditioned by the ideal AL preconditioner with the new Schur approximation  
 403  $\tilde{S}_{\gamma \text{ new}}$  on the grids with  $80 \times 40$  cells and  $160 \times 80$  cells. The fast convergence rate  
 404 confirms the prediction that the new Schur approximation  $\tilde{S}_{\gamma \text{ new}}$  produces a favorable  
 405 ideal AL preconditioner for the Krylov subspace solvers. In Figure 6 we observe that  
 406 larger values of  $\gamma$  result in a faster convergence rate on both grids. This observation  
 407 is analogous to that when applying the old Schur complement approximation  $\tilde{S}_{\gamma \text{ old}}$   
 408 in the ideal AL preconditioner with stable FEM, see [12] for instance. On the other  
 409 hand, an ill-conditioned  $Q_{\gamma}$  can arise from larger values of  $\gamma$  [32]. This indicates that  
 410 the value of  $\gamma$  can not be taken too large otherwise solving the momentum sub-system

411 with  $Q_\gamma$  can be very difficult. Results in Figure 6 indicate that the balanced value of  
 412  $\gamma$  involved in the ideal AL preconditioner with the new Schur approximation  $\tilde{S}_{\gamma \text{ new}}$   
 413 is  $\gamma = 1$  or  $O(1)$ .

414 Compared with the ideal AL preconditioner, the values of  $\gamma$  exhibit a different  
 415 influence on the spectrum of the preconditioned matrix by using the modified AL  
 416 preconditioner. For example, with  $\gamma = 100$  the smallest eigenvalue of  $\mathcal{P}_{MAL}^{-1}\mathcal{A}_\gamma$  is  
 417 two orders of magnitude smaller than  $\gamma = 0.01$  and  $\gamma = 1.0$ , as seen from the last  
 418 row of Figure 5. It appears that the optimal value of  $\gamma$ , which leads to the most  
 419 clustered eigenvalues of  $\mathcal{P}_{MAL}^{-1}\mathcal{A}_\gamma$ , is  $\gamma_{\text{opt}} = 1$ . Based on this observation we predict  
 420 that the fastest convergence rate of the Krylov subspace solvers preconditioned by the  
 421 modified AL preconditioner with  $\tilde{S}_{\gamma \text{ new}}$  can be obtained with  $\gamma_{\text{opt}} = 1$ .

422 The convergence rate of the Krylov subspace solvers preconditioned by the mod-  
 423 ified AL preconditioner with  $\tilde{S}_{\gamma \text{ new}}$  on the grids with  $80 \times 40$  cells and  $160 \times 80$  cells  
 424 is presented in Figure 7. We find out that  $\gamma_{\text{opt}} = 1$  results in the fastest convergence  
 425 rate on two grids and this confirms the prediction based on the spectrum analysis  
 426 from Figure 5. Compare two grids with  $160 \times 80$  cells and  $80 \times 40$  cells, it appears  
 427 that the optimal value  $\gamma_{\text{opt}} = 1$  is independent of mesh refinement. This property is  
 428 helpful in practice since one can carry out numerical experiments to determine  $\gamma_{\text{opt}}$   
 429 on coarse grids and then re-use it on finer grids.

430 In Table 1 we summarise the number of the Krylov subspace iterations precon-  
 431 ditioned by the AL preconditioners with the new Schur complement approximation  
 432  $\tilde{S}_{\gamma \text{ new}}$  and  $\gamma = 1$  on two grids. The value  $\gamma = 1$  is a balanced choice for the ideal AL  
 433 preconditioner and is the optimal choice for the modified AL preconditioner. As seen,  
 434 for this considered turbulent case the new Schur complement approximation  $\tilde{S}_{\gamma \text{ new}}$   
 435 does not make the AL preconditioners independent of mesh refinement. This moti-  
 436 vates a further study targeting at mesh independence, which is planned as a research  
 437 direction in future.

Table 1: Turbulent FP: the number of GMRES iterations (no restart) preconditioned  
 by the AL preconditioners with the new Schur approximation  $\tilde{S}_{\gamma \text{ new}}$  and  $\gamma = 1$  on  
 two grids.

Grid	$80 \times 40$ cells	$160 \times 80$ cells
$\mathcal{P}_{MAL}$ :	140	246
$\mathcal{P}_{IAL}$ :	132	245

438 On the other hand, the proposal of the new Schur complement approximation  
 439  $\tilde{S}_{\gamma \text{ new}}$  is a big contribution to the development of AL preconditioners in the context  
 440 of turbulent calculations. This is clearly seen from Figure 8 where the Krylov subspace  
 441 solver converges very slowly when applying the old Schur complement approximation  
 442  $\tilde{S}_{\gamma \text{ old}}$  in the modified AL preconditioner. To understand this slow convergence the  
 443 extreme eigenvalues of  $\mathcal{P}_{MAL}^{-1}\mathcal{A}_\gamma$  with  $\tilde{S}_{\gamma \text{ old}}$  on the grid with  $80 \times 40$  cells are presented  
 444 in Figure 9. We see that the smallest eigenvalues are quite close to zero for all tested  
 445 values of  $\gamma$ , which degrades the efficiency of the Krylov subspace solver considerably.  
 446 Among the tested values of  $\gamma$ , Figure 9 shows that  $\gamma = 1$  results in a relatively clustered  
 447 spectrum. Based on this observation we expect that the optimal value  $\gamma_{\text{opt}} = 1$  leads  
 448 to the fastest convergence when using the old Schur complement approximation  $\tilde{S}_{\gamma \text{ old}}$   
 449 in the modified AL preconditioner. However, the number of the Krylov subspace  
 450 iterations preconditioned by  $\mathcal{P}_{MAL}$  with  $\tilde{S}_{\gamma \text{ old}}$  and  $\gamma_{\text{opt}} = 1$  is over than 5000 as  
 451 seen from Figure 8. Compared with 140 Krylov subspace iterations preconditioned

452 by  $\mathcal{P}_{MAL}$  with  $\tilde{S}_{\gamma \text{ new}}$  and  $\gamma_{\text{opt}} = 1$ , we clearly show that the new Schur complement  
 453 approximation  $\tilde{S}_{\gamma \text{ new}}$  proposed in this paper significantly improves the performance  
 454 of the AL preconditioners on the turbulent FP case.

455 We also present the spectrum of the eigenvalues and convergence rate by using  
 456 the SIMPLE preconditioner. These results are compared with the modified AL pre-  
 457 conditioner with the new Schur complement approximation  $\tilde{S}_{\gamma \text{ new}}$  and  $\gamma_{\text{opt}} = 1$ . The  
 458 comparison given in Figure 10 illustrates that on the grid with  $80 \times 40$  cells the small-  
 459 est eigenvalues are nearly the same for both preconditioners. However, the SIMPLE  
 460 preconditioner leads to a larger ratio between the largest and smallest magnitude of  
 461 the eigenvalues, which means that the spectrum of the eigenvalues is less clustered  
 462 compared to the modified AL preconditioner. Therefore, a faster convergence rate of  
 463 the Krylov subspace solvers is expected by applying the modified AL preconditioner.  
 464 Table 2 presents the number of GMRES iterations preconditioned by the SIMPLE  
 465 preconditioner and the modified AL preconditioner with  $\tilde{S}_{\gamma \text{ new}}$  and  $\gamma_{\text{opt}} = 1$  on two  
 466 grids. Results in Table 2 illustrate that the number of the Krylov subspace itera-  
 467 tions increase by a factor 1.7 by using the modified AL preconditioner with  $\tilde{S}_{\gamma \text{ new}}$   
 468 and  $\gamma_{\text{opt}} = 1$ . The increasing factor is 2.2 when using the SIMPLE preconditioner.  
 469 The smaller increasing factor allows a more apparent advantage of the modified AL  
 470 preconditioner with  $\tilde{S}_{\gamma \text{ new}}$  in terms of the reduced number of the Krylov subspace  
 471 iterations with mesh refinement, which foresees the overall advantage in terms of total  
 472 wall-clock time on fine enough grids.

Table 2: Turbulent FP: the number of GMRES iterations (no restart) preconditioned  
 by the modified AL preconditioner  $\mathcal{P}_{MAL}$  with the new Schur approximation  $\tilde{S}_{\gamma \text{ new}}$   
 and  $\gamma_{\text{opt}} = 1$ , and the SIMPLE preconditioner  $\mathcal{P}_{SIMPLE}$  on two grids.

Grid	$80 \times 40$ cells	$160 \times 80$ cells
$\mathcal{P}_{MAL}$ :	140	246
$\mathcal{P}_{SIMPLE}$ :	180	382

473 **5.4. Numerical experiments on the turbulent BFS case.** On the calcula-  
 474 tions of turbulent BFS case, we further assess the new Schur complement approxima-  
 475 tion  $\tilde{S}_{\gamma \text{ new}}$  applied in the modified AL preconditioner and present the convergence  
 476 rate of the Krylov subspace solver in Figure 11 (a). As seen, the utilisation of  $\tilde{S}_{\gamma \text{ new}}$   
 477 produces quite a fast convergence rate in the turbulent BFS case too. Among the  
 478 considered values of  $\gamma$ , it appears that  $\gamma_{\text{opt}} = 0.1$  results in the fastest convergence  
 479 rate on the turbulent BFS case. Consider  $\gamma_{\text{opt}} = 1$  on the turbulent FP test, we find  
 480 out that the optimal value of  $\gamma$  which results in the best performance of the modified  
 481 AL preconditioner with the new Schur complement approximation  $\tilde{S}_{\gamma \text{ new}}$  is weakly  
 482 problem dependent.

483 Comparable with the turbulent FP case, on the turbulent BFS test we also see the  
 484 faster convergence rate achieved by using the modified AL preconditioner with  $\tilde{S}_{\gamma \text{ new}}$   
 485 than the SIMPLE preconditioner. Comparison in Figure 11 (a) shows that the number  
 486 of the Krylov subspace iterations preconditioned by the modified AL preconditioner  
 487 with  $\tilde{S}_{\gamma \text{ new}}$  and  $\gamma_{\text{opt}} = 0.1$  is nearly half of that by using the SIMPLE preconditioner.  
 488 Based on the result with mesh refinement on the turbulent FP case (see Table 2), it  
 489 is reasonable to expect that on turbulent BFS test less Krylov subspace iterations  
 490 preconditioned by the modified AL preconditioner with  $\tilde{S}_{\gamma \text{ new}}$  will convert to a time  
 491 advantage over the SIMPLE preconditioner on fine grids.

492 To illustrate the improvement arising from the utilisation of the new Schur com-

493 plement approximation  $\tilde{S}_{\gamma \text{ new}}$ , in Figure 11 (b) we present the convergence rate  
 494 preconditioned by the modified AL preconditioner with the old Schur complement  
 495 approximation  $\tilde{S}_{\gamma \text{ old}}$ . The fastest convergence rate with  $\tilde{S}_{\gamma \text{ old}}$  is obtained with  
 496  $\gamma_{\text{opt}} = 1$  and other values of  $\gamma$  can not make the solution procedure converged to  
 497 the desired tolerance within the maximal 1000 iterations. The fastest convergence  
 498 rate with  $\tilde{S}_{\gamma \text{ old}}$  and  $\gamma_{\text{opt}} = 1$  is about eight times slower than  $\tilde{S}_{\gamma \text{ new}}$  with  $\gamma_{\text{opt}} = 0.1$ .  
 499 The turbulent BFS case is another example to illustrate the advantage of the new  
 500 Schur approximation  $\tilde{S}_{\gamma \text{ new}}$  over the old one  $\tilde{S}_{\gamma \text{ old}}$  in the turbulent context.

501 For a comprehensive comparison, in Table 3 we summarise the number of the  
 502 Krylov subspace iterations accelerated by different preconditioners. Since we have  
 503 observed the mesh dependence of the AL preconditioners with the new Schur approx-  
 504 imation  $\tilde{S}_{\gamma \text{ new}}$  on the turbulent FP case, we expect an analogous behaviour on the  
 505 turbulent BFS case. The planned future research includes the improvement which  
 506 allows the robustness with respect to mesh refinement on turbulent calculations.

Table 3: Turbulent BFS: the number of GMRES iterations (no restart) preconditioned by the AL preconditioners with different Schur complement approximations and different values of  $\gamma$ , and the SIMPLE preconditioner. The grid with 9600 cells is used.

$\gamma$	0.01	0.1	1
$\mathcal{P}_{IAL}$ with $\tilde{S}_{\gamma \text{ new}}$ :	133	103	96
$\mathcal{P}_{MAL}$ with $\tilde{S}_{\gamma \text{ new}}$ :	134	104	111
$\mathcal{P}_{MAL}$ with $\tilde{S}_{\gamma \text{ old}}$ :	> 1000	> 1000	791
$\mathcal{P}_{SIMPLE}$ :	199		

507 **5.5. Numerical experiments on the laminar FP case.** The modified AL  
 508 preconditioner is often utilised due to the reduced complexity of solving the sub-  
 509 system with  $\tilde{Q}_{\gamma}$ , compared to  $Q_{\gamma}$  involved in the ideal AL preconditioner. The extreme  
 510 eigenvalues of  $\mathcal{P}_{MAL}^{-1} \mathcal{A}_{\gamma}$  with the new Schur approximation  $\tilde{S}_{\gamma \text{ new}}$  are shown in Figure  
 511 13. There are two observations to be made. Firstly, for moderate values of  $\gamma$ , e.g.,  $\gamma \in$   
 512  $[0.01, 0.1]$ , the smallest eigenvalues are far away from zero. Secondly,  $\gamma = 0.1$  results  
 513 in the smallest ratio between the largest and smallest magnitude of the eigenvalues.  
 514 Thus, we expect that the optimal value of  $\gamma$  is  $\gamma_{\text{opt}} = 0.1$  for the laminar FP case.  
 515 The prediction is confirmed by Figure 12 which illustrates that  $\gamma_{\text{opt}} = 0.1$  results in  
 516 the fastest convergence rate among other tested values of  $\gamma$ .

517 In [32] we find out that for the laminar FP case the optimal value of  $\gamma$  for the  
 518 old Schur approximation  $\tilde{S}_{\gamma \text{ old}}$  is  $\gamma_{\text{opt}} = 400$ . Seen from Table 4, on the laminar  
 519 FP case the modified AL preconditioner with the new Schur approximation  $\tilde{S}_{\gamma \text{ new}}$   
 520 and  $\gamma_{\text{opt}} = 0.1$  reduces the number of the Krylov subspace iterations by factors 14.6  
 521 and 2.2, compared to the old Schur approximation  $\tilde{S}_{\gamma \text{ old}}$  with  $\gamma_{\text{opt}} = 400$  and the  
 522 SIMPLE preconditioner, respectively. The above numerical results clearly show that  
 523 the new Schur complement approximation  $\tilde{S}_{\gamma \text{ new}}$  proposed in this paper significantly  
 524 improves the performance of the AL preconditioner for laminar flows too.

Table 4: Laminar FP: the number of GMRES iterations (no restart) preconditioned the modified AL preconditioner with two Schur complement approximations and their corresponding optimal values of  $\gamma$ , and the SIMPLE preconditioner. The grid with  $64 \times 64$  cells is used.

$\mathcal{P}_{MAL}$ with $\tilde{S}_{\gamma \text{ new}}$ and $\gamma_{\text{opt}} = 0.1$	$\mathcal{P}_{MAL}$ with $\tilde{S}_{\gamma \text{ old}}$ and $\gamma_{\text{opt}} = 400$	$\mathcal{P}_{SIMPLE}$
83	1200	183

525 In the previous work [32] we set the stopping tolerance for the linear system to be  
 526  $10^{-3}$  on the laminar FP case and compare the modified AL preconditioner with the  
 527 old Schur complement approximation and the SIMPLE preconditioner in terms of the  
 528 number of the Krylov subspace iterations. This comparison is executed based on the  
 529 chosen stopping tolerance which balances the linear and nonlinear solvers. Since the  
 530 nonlinear solver is not the focus of this paper, it is reasonable to solve the linear system  
 531 to the machine accuracy so that a comprehensive evaluation of the proposed new Schur  
 532 complement approximation in the AL preconditioner and a complete comparison with  
 533 the old Schur complement approximation and the SIMPLE preconditioner can be  
 534 obtained. In this sense, the results in Table 4, regarding the number of the Krylov  
 535 subspace iterations preconditioned by the modified AL preconditioner with the old  
 536 Schur complement approximation and the SIMPLE preconditioner, supplement the  
 537 previous work [32].

538 **5.6. Comparisons between the turbulent and laminar calculations.** Fi-  
 539 nally we put the turbulent and laminar results together in Table 5 for a comparison.  
 540 Consider the modified AL preconditioner with the new Schur approximation  $\tilde{S}_{\gamma \text{ new}}$   
 541 and the optimal value  $\gamma_{\text{opt}}$ , we see that the number of the Krylov subspace iterations  
 542 is quite acceptable for all tested cases. This means that the new Schur complement  
 543 approximation proposed in this paper makes the AL preconditioner robust with re-  
 544 spect to the mesh anisotropy and physical parameter variation, e.g. the variation of  
 545 the viscosity. Regarding the optimal value of  $\gamma$ , it lies in the interval  $[0.1, 1]$  for all  
 546 tests when applying the new Schur complement approximation in the modified AL  
 547 preconditioner. This interval is much more clustered than that when using the old  
 548 Schur complement approximation. This means that the optimal value  $\gamma_{\text{opt}}$  is easier  
 549 to determine and weakly problem dependent for the new variant. Regarding the in-  
 550 fluence of  $\gamma$  on the convergence, we observe that by using the new Schur complement  
 551 approximation the variation of the convergence rate arising from different values of  $\gamma$   
 552 is much less than that with the old approximation. See Figure 11 on the turbulent  
 553 BFS case for instance. This illustrates that the new AL variant is less sensitive to the  
 554 values of  $\gamma$ . Besides, the advantage of the new Schur approximation over the old one is  
 555 clearly exhibited in terms of the significantly reduced number of the Krylov subspace  
 556 iterations on all cases. This means that new Schur approximation can considerably  
 557 improve the efficiency of the AL preconditioner for both turbulent and laminar cal-  
 558 culations. Although the number of the Krylov subspace iterations by applying the  
 559 modified AL preconditioner with new Schur approximation and the optimal value of  
 560  $\gamma$  is less than the SIMPLE preconditioner, the benefit in terms of the total wall-clock  
 561 time needs the further assessment due to the heavier cost of the AL preconditioner  
 562 presented in Section 4. This is included in the future research plan.

Table 5: The number of GMRES iterations (no restart) accelerated by different preconditioners on different tests. The grids with  $80 \times 40$  cells, 9600 cells and  $64 \times 64$  cells are used for the turbulent FP, turbulent BFS and laminar FP cases respectively.

	turbulent FP	turbulent BFS	laminar FP
$\mathcal{P}_{MAL}$ with $\tilde{S}_{\gamma \text{ new}}$			
$\gamma_{\text{opt}}$ :	1	0.1	0.1
iterations:	140	104	83
$\mathcal{P}_{MAL}$ with $\tilde{S}_{\gamma \text{ old}}$			
$\gamma_{\text{opt}}$ :	1	1	400
iterations:	> 5000	791	1200
$\mathcal{P}_{SIMPLE}$			
iterations:	180	199	183

563 **6. Conclusion and future work.** In this paper, we have considered the extension  
 564 of the AL preconditioner in the context of the stabilized finite volume methods  
 565 to both laminar flow governed by the Navier-Stokes equations and turbulent flow gov-  
 566 erned by the Reynolds-Averaged Navier-Stokes (RANS) equations with eddy-viscosity  
 567 turbulence model.

568 We find out that the straightforward application of the AL preconditioner to  
 569 the RANS equations yields disappointing results and therefore proposed a new Schur  
 570 complement approximation which leads to a variant of the AL preconditioner. The ap-  
 571 proach is to substitute the approximation of the Schur complement from the SIMPLE  
 572 preconditioner into the inverse of the Schur complement for the AL preconditioner.  
 573 Without the contradictory requirements in the old approximation, the new Schur  
 574 complement approximation makes the new AL variant less sensitive to the choice of  
 575  $\gamma$  and weakly problem dependent.

576 To evaluate the new variant of the AL preconditioner, we consider the solution  
 577 of the linear system obtained at the 30th nonlinear iteration for three cases: laminar  
 578 and turbulent boundary-layer flow over a flat plate on grids with large aspect ratios,  
 579 and turbulent flow over a backward-facing step in a channel. The backward-facing  
 580 step flow is more complicated than the flat-plate flow as it features separation, a free  
 581 shear-layer and reattachment. The new variant of the AL preconditioner significantly  
 582 speeds up the convergence rate of the Krylov subspace solvers for both turbulent and  
 583 laminar cases. Spectral analysis of the preconditioned systems explains the observed  
 584 difference. Like the SIMPLE preconditioner, the new AL variant avoids the clustering  
 585 of the smallest eigenvalues near zero. At the same time, the largest eigenvalues by  
 586 applying the the new AL variant are significantly smaller than the SIMPLE precondi-  
 587 tioner. As a consequence, the new variant of the AL preconditioner outperforms the  
 588 considered preconditioners in terms of the number of the Krylov subspace iterations.  
 589 The matrices and right-hand side vectors used in this paper are publicly available  
 590 on the website [18]. This makes the research reproducible and the comparison with  
 591 other preconditioning techniques easier.

592 We present a basic cost model to compare the new variant with others, including  
 593 the SIMPLE preconditioner which is well established for the RANS equations. The  
 594 heavier cost of the new AL variant can be payed off with less Krylov subspace iter-  
 595 ations which is seen in this paper. However, our test cases so far have been carried  
 596 out on the modest grid sizes that allow the matrices to be exported and analyzed in  
 597 Matlab. Future work is planned on the assessment of the new AL variant on larger  
 598 grid sizes to show the benefit in terms of the reduced total wall-clock time. In this  
 599 paper we observe that the new AL variant is not mesh independent. Another planned

600 future research is on the improvement which allows the robustness with respect to  
601 mesh refinement.

Fig. 4: Turbulent FP: the ten smallest (left) and largest (right) eigenvalues of  $\mathcal{P}_{IAL}^{-1}\mathcal{A}_\gamma$  with the new Schur approximation  $\tilde{\mathcal{S}}_{\gamma \text{ new}}$  and different values of  $\gamma$ . The grid with  $80 \times 40$  cells is used.

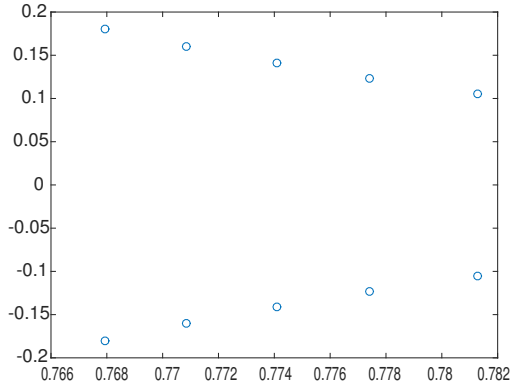
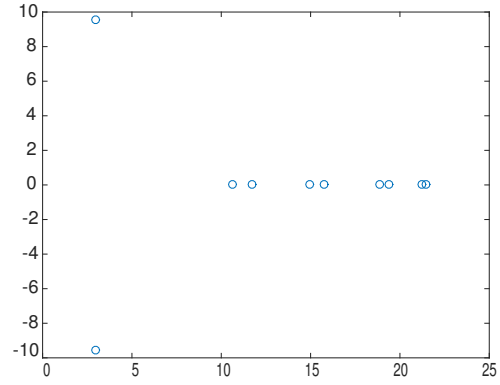
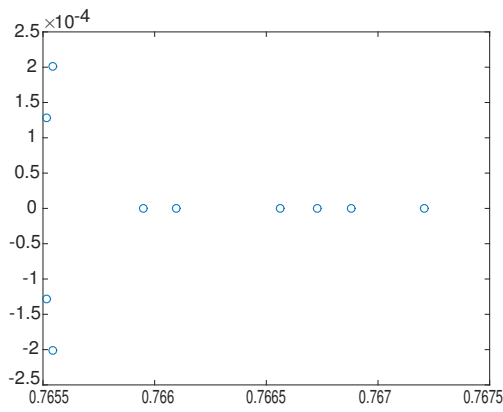
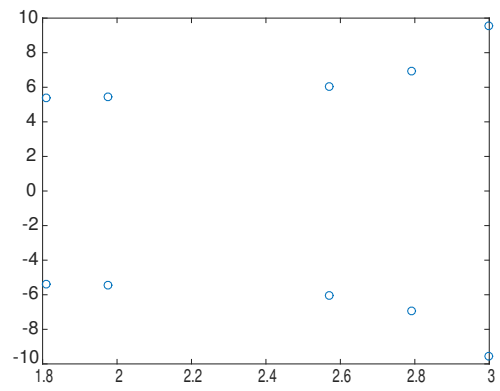
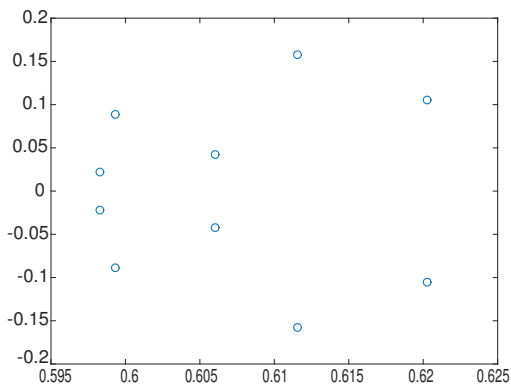
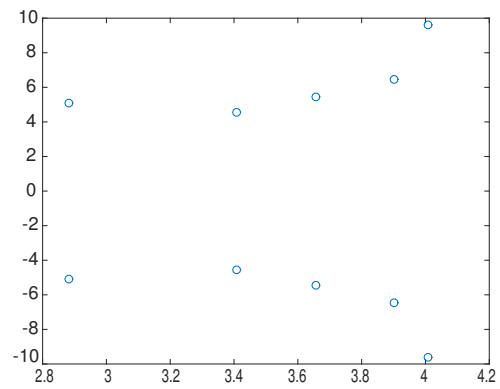
(a)  $\gamma = 0.01$ (b)  $\gamma = 0.01$ (c)  $\gamma = 1$ (d)  $\gamma = 1$ (e)  $\gamma = 100$ (f)  $\gamma = 100$

Fig. 5: Turbulent FP: the ten smallest (left) and largest (right) eigenvalues of  $\mathcal{P}_{MAL}^{-1}\mathcal{A}_\gamma$  with the new Schur approximation  $\tilde{\mathcal{S}}_\gamma$  and different values of  $\gamma$ . The grid with  $80 \times 40$  cells is used.

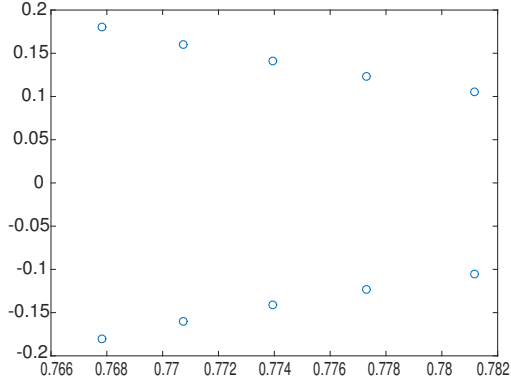
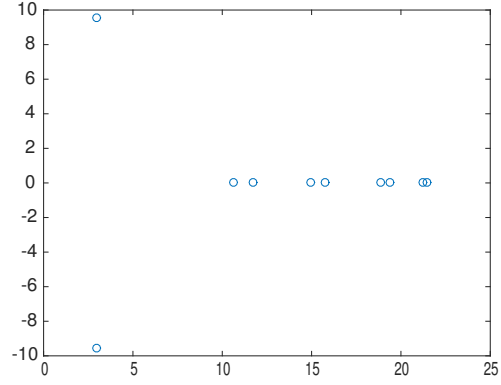
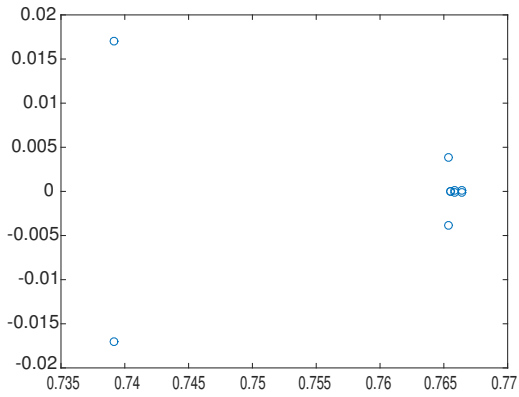
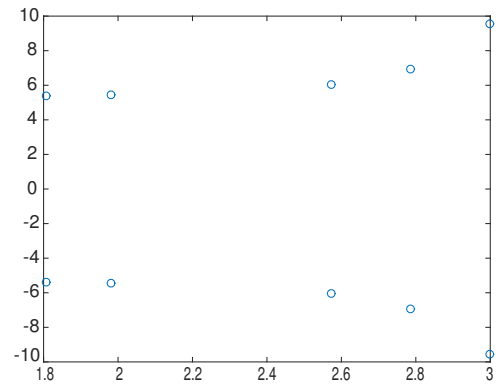
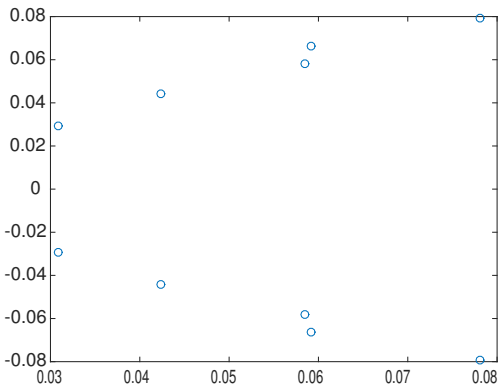
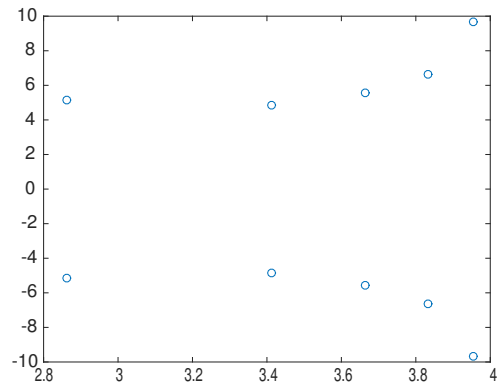
(a)  $\gamma = 0.01$ (b)  $\gamma = 0.01$ (c)  $\gamma = 1$ (d)  $\gamma = 1$ (e)  $\gamma = 100$ (f)  $\gamma = 100$

Fig. 6: Turbulent FP: the convergence of GMRES (no restart) preconditioned by the ideal AL preconditioner  $\mathcal{P}_{IAL}$  with the new Schur approximation  $\tilde{S}_{\gamma \text{ new}}$  on the grids with  $80 \times 40$  cells (left) and  $160 \times 80$  cells (right).

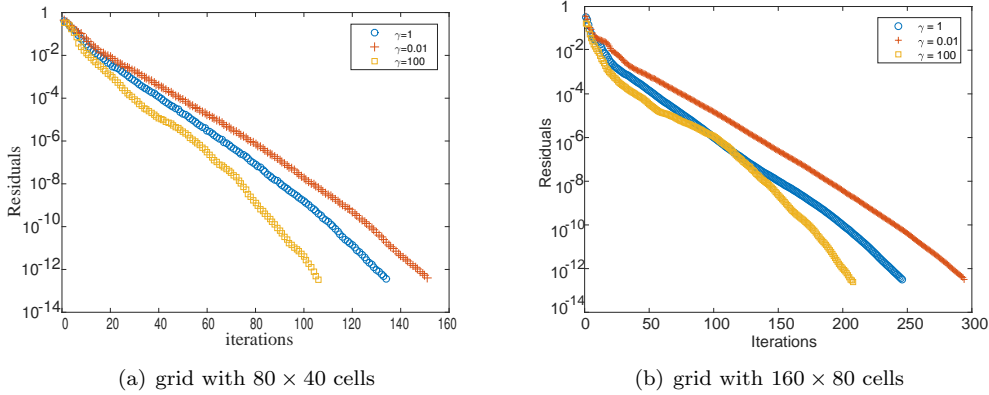


Fig. 7: Turbulent FP: the convergence of GMRES (no restart) preconditioned by the modified AL preconditioner  $\mathcal{P}_{MAL}$  with the new Schur approximation  $\tilde{S}_{\gamma \text{ new}}$  on the grids with  $80 \times 40$  cells (left) and  $160 \times 80$  cells (right).

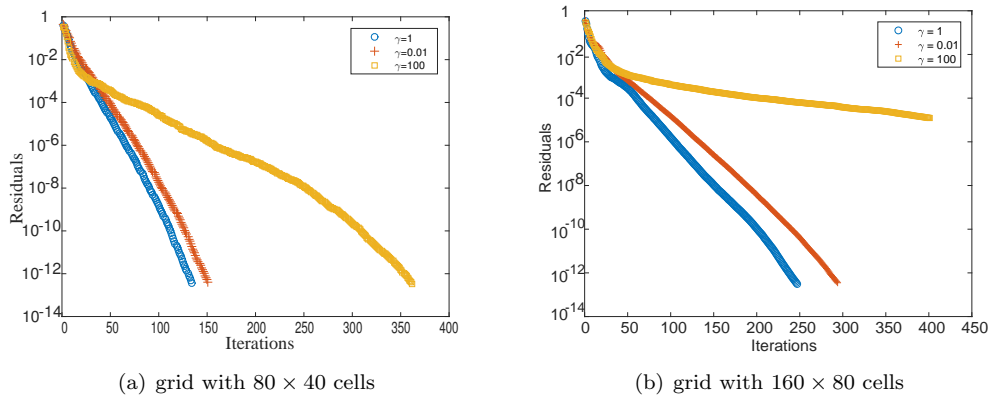


Fig. 8: Turbulent FP: the convergence of GMRES (no restart) preconditioned by the modified AL preconditioner  $\mathcal{P}_{MAL}$  with the old Schur approximation  $\tilde{S}_{\gamma \text{ old}}$  and  $\gamma_{\text{opt}} = 1$ . The grid with  $80 \times 40$  cells is used.

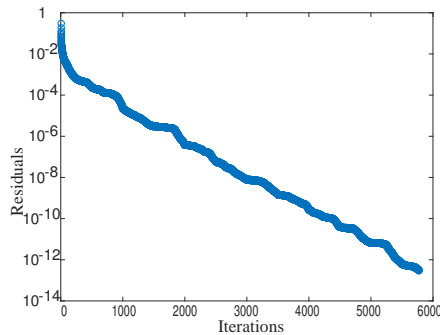


Fig. 9: Turbulent FP: the ten smallest (left) and largest (right) eigenvalues of  $\mathcal{P}_{MAL}^{-1}\mathcal{A}_\gamma$  with the old Schur approximation  $\tilde{\mathcal{S}}_{\gamma \text{ old}}$  and different values of  $\gamma$ . The grid with  $80 \times 40$  cells is used.

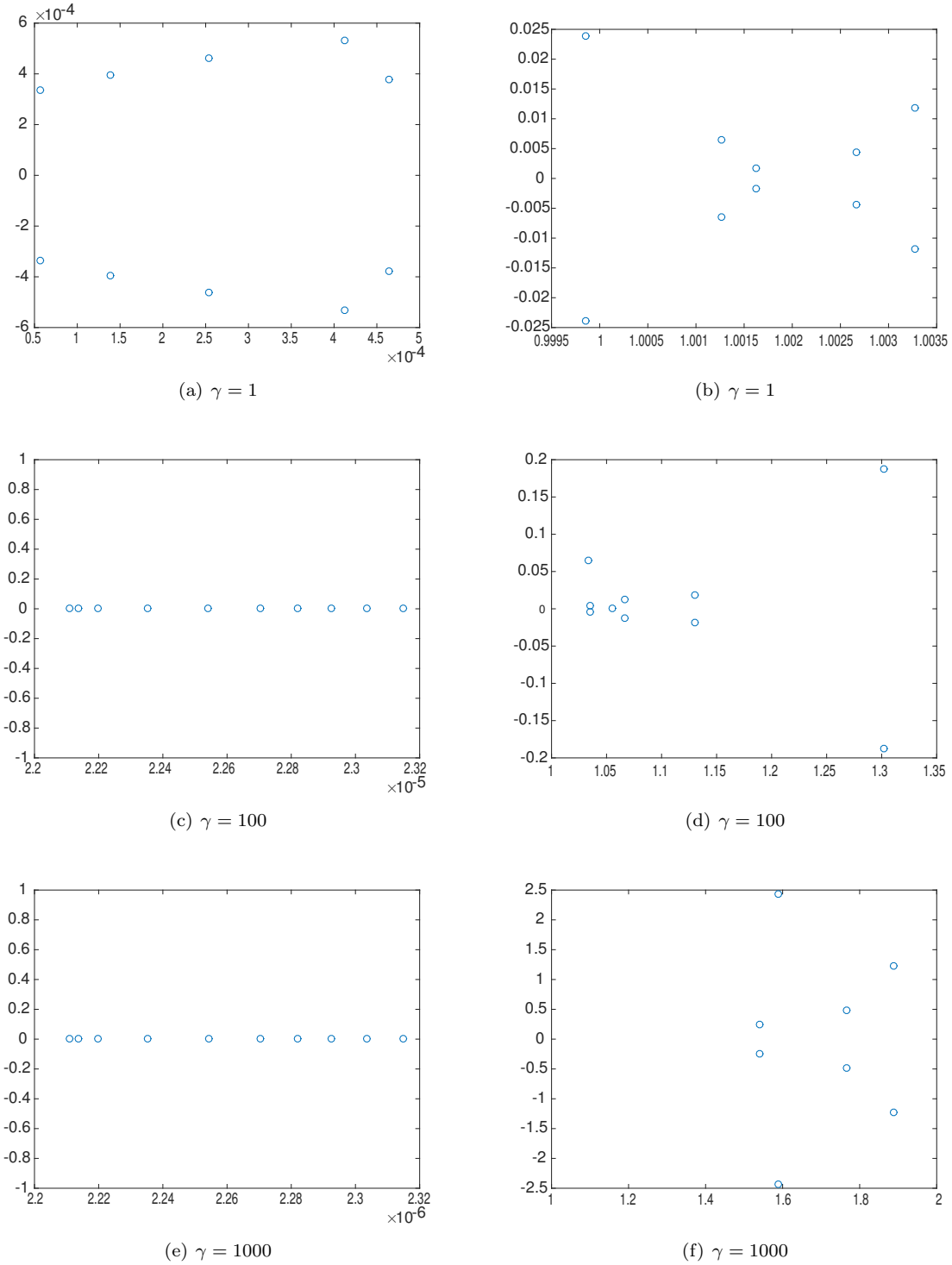


Fig. 10: Turbulent FP: the ten smallest (left) and largest (right) eigenvalues of  $\mathcal{P}_{MAL}^{-1}\mathcal{A}_\gamma$  with the new Schur approximation  $\tilde{S}_\gamma$  new and  $\gamma_{\text{opt}} = 1$ , and of  $\mathcal{P}_{SIMPLE}^{-1}\mathcal{A}$ . The grid with  $80 \times 40$  cells is used.

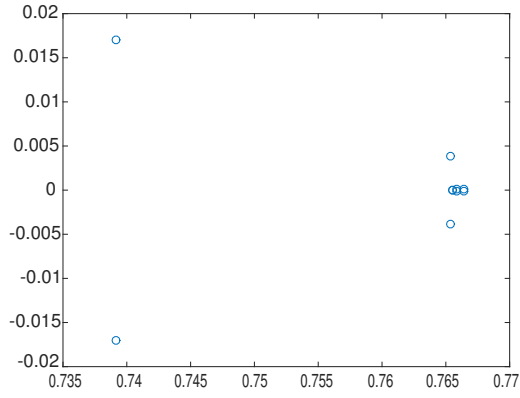
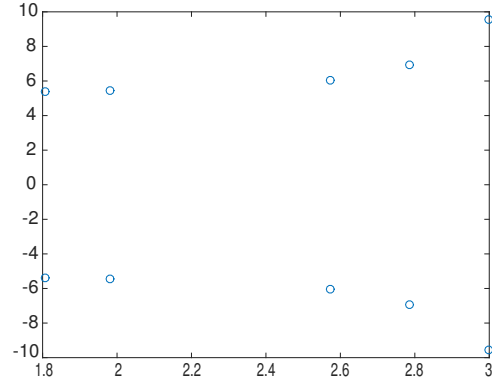
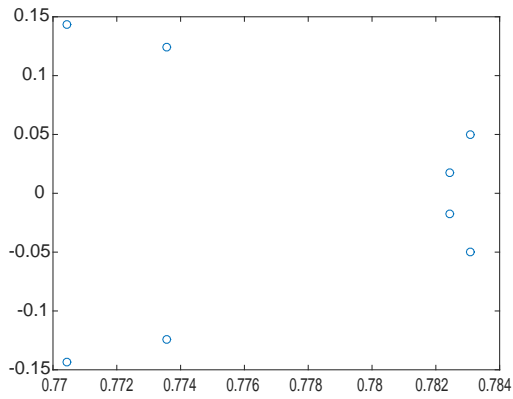
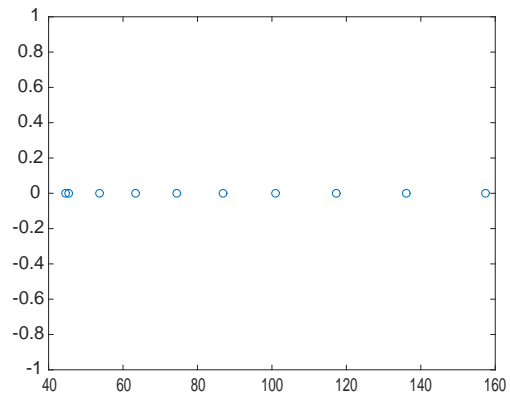
(a)  $\mathcal{P}_{MAL}^{-1}\mathcal{A}_\gamma$ (b)  $\mathcal{P}_{MAL}^{-1}\mathcal{A}_\gamma$ (c)  $\mathcal{P}_{SIMPLE}^{-1}\mathcal{A}$ (d)  $\mathcal{P}_{SIMPLE}^{-1}\mathcal{A}$

Fig. 11: Turbulent BFS: the convergence of GMRES (no restart) preconditioned by the modified AL preconditioner  $\mathcal{P}_{MAL}$  with the new Schur approximation  $\tilde{S}_\gamma$  new and the SIMPLE preconditioner (left), and the modified AL preconditioner  $\mathcal{P}_{MAL}$  with the old Schur approximation  $\tilde{S}_\gamma$  old (right). The grid with 9600 cells is used.

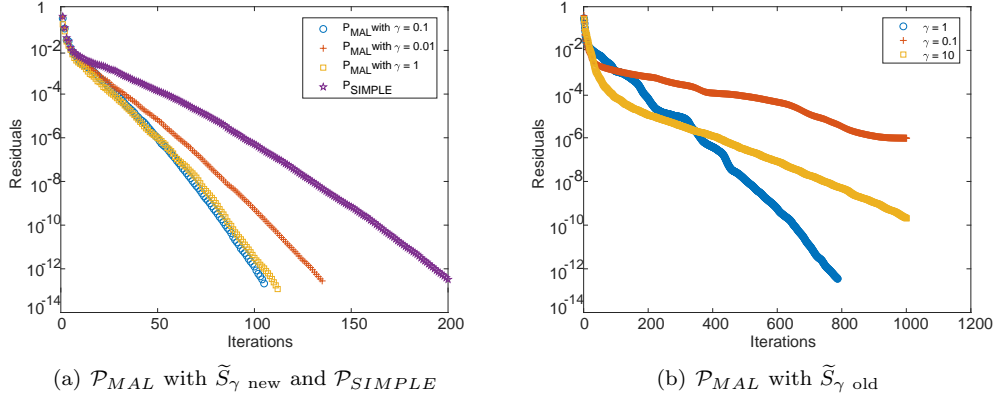


Fig. 12: Laminar FP: the convergence of GMRES (no restart) preconditioned by the modified AL preconditioner with the new Schur complement approximation  $\tilde{S}_\gamma$  new and different values of  $\gamma$ . The grid with  $64 \times 64$  cells is used.

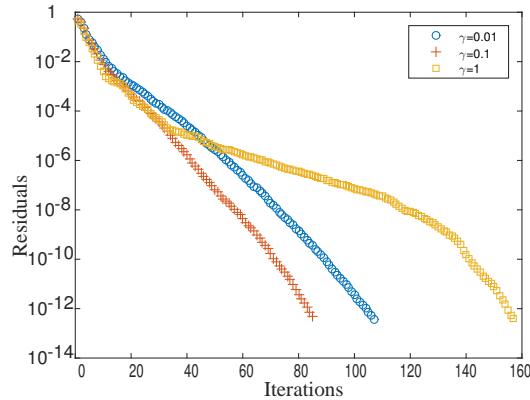
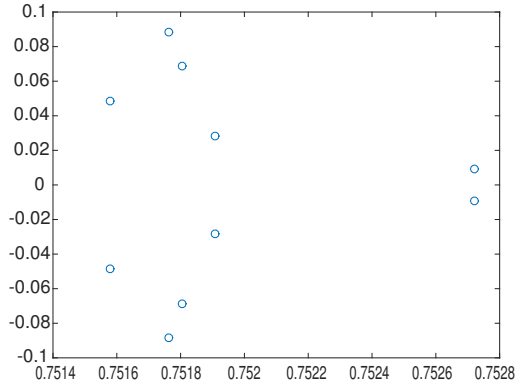
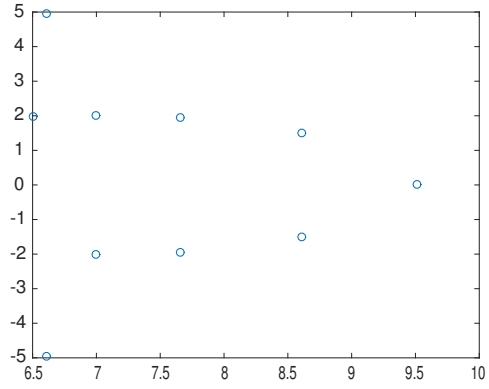
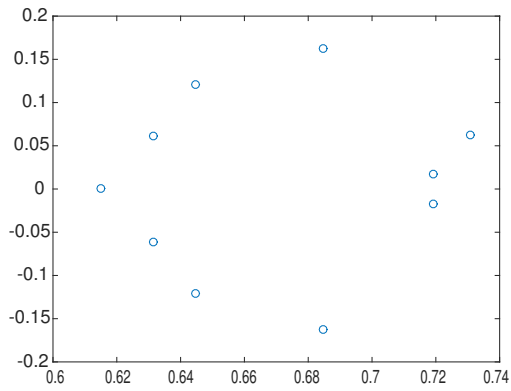
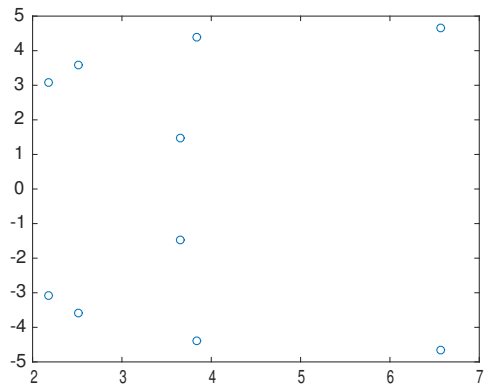
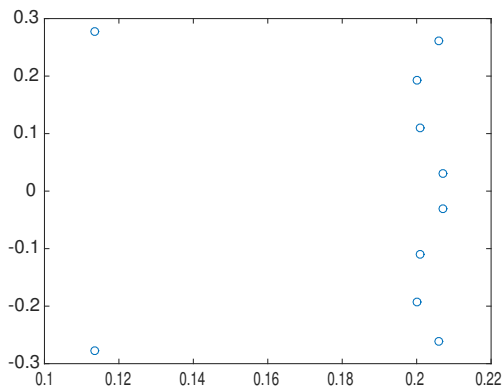
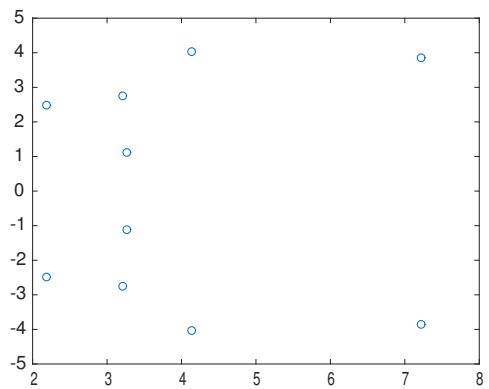


Fig. 13: Laminar FP: the ten smallest (left) and largest (right) eigenvalues of  $\mathcal{P}_{MAL}^{-1}\mathcal{A}_\gamma$  with the new Schur approximation  $\tilde{\mathcal{S}}_{\gamma \text{ new}}$  and different values of  $\gamma$ . The grid with  $64 \times 64$  cells is used.

(a)  $\gamma = 0.01$ (b)  $\gamma = 0.01$ (c)  $\gamma = 0.1$ (d)  $\gamma = 0.1$ (e)  $\gamma = 1$ (f)  $\gamma = 1$

602

## REFERENCES

- 603 [1] M. BENZI, G. GOLUB, AND J. LIESEN, Numerical solution of saddle point problems, Acta  
604 numerica, 14 (2005), pp. 1–137.
- 605 [2] M. BENZI AND M. OLSHANSKII, An augmented Lagrangian-based approach to the Oseen  
606 problem, SIAM Journal on Scientific Computing, 28 (2006), pp. 2095–2113.
- 607 [3] M. BENZI, M. OLSHANSKII, AND Z. WANG, Modified augmented Lagrangian preconditioners for  
608 the incompressible Navier-Stokes equations, International Journal for Numerical Methods  
609 in Fluids, 66 (2011), pp. 486–508.
- 610 [4] M. BENZI AND Z. WANG, Analysis of augmented Lagrangian-based preconditioners for the  
611 steady incompressible Navier-Stokes equations, SIAM Journal on Scientific Computing, 33  
612 (2011), pp. 2761–2784.
- 613 [5] M. BENZI AND Z. WANG, A parallel implementation of the modified augmented Lagrangian  
614 preconditioner for the incompressible Navier-Stokes equations, Numerical Algorithms, 64  
615 (2013), pp. 73–84.
- 616 [6] D. DRIVER AND H. SEEGMILLER, Features of a reattaching turbulent shear layer in divergent  
617 channel flow, AIAA Journal, 23 (1985), pp. 163–171.
- 618 [7] L. EÇA, G. VAZ, AND M. HOEKSTRA, A verification and validation exercise for the flow over a  
619 backward facing step, in Proceedings of the Fifth European Conference on Computational  
620 Fluid Dynamics ECCOMAS CFD 2010, J. Pereira and A. Sequeria, eds., 2010. June 14 –  
621 17, Lisbon, Portugal.
- 622 [8] H. ELMAN, V. HOWLE, J. SHADID, R. SHUTTLEWORTH, AND R. TUMINARO, Block  
623 preconditioners based on approximate commutators, SIAM Journal on Scientific Com-  
624 puting, 27 (2006), pp. 1651–1668.
- 625 [9] H. ELMAN, D. SILVESTER, AND A. WATHEN, Finite elements and fast iterative solvers: with  
626 applications in incompressible fluid dynamics, Oxford University Press, 2014.
- 627 [10] ERCOFTAC, Classic Collection Database, [http://www.ercofac.org/products\\_and\\_services/  
628 classic\\_collection\\_database/](http://www.ercofac.org/products_and_services/classic_collection_database/).
- 629 [11] J. FERZIGER AND M. PERIC, Computational methods for fluid dynamics, Springer Science &  
630 Business Media, 2012.
- 631 [12] X. HE, M. NEYTICHEVA, AND C. VUIK, On an augmented lagrangian-based preconditioning of  
632 Oseen type problems, BIT Numerical Mathematics, 51 (2011), pp. 865–888.
- 633 [13] D. KAY, D. LOGHIN, AND A. WATHEN, A preconditioner for the steady-state Navier-Stokes  
634 equations, SIAM Journal on Scientific Computing, 24 (2002), pp. 237–256.
- 635 [14] C. KLAIJ, On the stabilization of finite volume methods with co-located variables for  
636 incompressible flow, Journal of Computational Physics, 297 (2015), pp. 84–89.
- 637 [15] C. KLAIJ, X. HE, AND C. VUIK, On the design of block preconditioners for maritime engineering,  
638 in Proceedings of the Seventh International Conference on Computational Methods in  
639 Marine Engineering MARINE, M. Visonneau, P. Queutey, and D. L. Touzé, eds., 2017.  
640 May 15 – 17, Nantes, France.
- 641 [16] C. KLAIJ AND C. VUIK, SIMPLE-type preconditioners for cell-centered, colocated finite volume  
642 discretization of incompressible Reynolds-averaged Navier-Stokes equations, International  
643 Journal for Numerical Methods in Fluids, 71 (2013), pp. 830–349.
- 644 [17] C. LI AND C. VUIK, Eigenvalue analysis of the SIMPLE preconditioning for incompressible  
645 flow, Numerical Linear Algebra with Applications, 11 (2004), pp. 511–523.
- 646 [18] MARITIME RESEARCH INSTITUTE NETHERLANDS, ReFRESCO linear systems, [http://www.  
647 refresco.org/publications/data-sharing/linear-systems/](http://www.refresco.org/publications/data-sharing/linear-systems/).
- 648 [19] MARITIME RESEARCH INSTITUTE NETHERLANDS, ReFRESCO Web page, [http://www.refresco.  
649 org](http://www.refresco.org).
- 650 [20] F. MENTER, Two-equation eddy-viscosity turbulence models for engineering applications, AIAA  
651 Journal, 32 (1994), pp. 1598–1605.
- 652 [21] T. MILLER AND F. SCHMIDT, Use of a pressure-weighted interpolation method for the solution  
653 of the incompressible Navier-Stokes equations on a nonstaggered grid system, Numerical  
654 Heat Transfer, Part A: Applications, 14 (1988), pp. 213–233.
- 655 [22] M. OLSHANSKII AND E. TYRTYSHNIKOV, Iterative methods for linear systems: theory and  
656 applications, SIAM, 2014.
- 657 [23] P. PATANKAR, Numerical heat transfer and fluid flow, McGraw-Hill, New York, 1980.
- 658 [24] J. PESTANA AND A. WATHEN, Natural preconditioning and iterative methods for saddle point  
659 systems, SIAM Review, 57 (2015), pp. 71–91.
- 660 [25] D. RIJPKEMA, Flat plate in turbulent flow, Tech. Report 23279-1-RD, Maritime Research In-  
661 stitute Netherlands, 2009.
- 662 [26] Y. SAAD, V. DER VORST, AND A. HENK, Iterative solution of linear systems in the 20th century,

- 663           Journal of Computational and Applied Mathematics, 123 (2000), pp. 1–33.  
664 [27] A. SEGAL, M. UR REHMAN, AND C. VUIK, Preconditioners for incompressible Navier-Stokes  
665 solvers, Numerical Mathematics: Theory, Methods and Applications, 3 (2010), pp. 245–  
666 275.
- 667 [28] D. SILVESTER, H. ELMAN, D. KAY, AND A. WATHEN, Efficient preconditioning of the linearized  
668 Navier-Stokes equations for incompressible flow, Journal of Computational and Applied  
669 Mathematics, 128 (2001), pp. 261–279.
- 670 [29] C. VUIK, A. SAGHIR, AND G. BOERSTOEL, The Krylov accelerated SIMPLE(R) method for flow  
671 problems in industrial furnaces, International Journal for Numerical methods in fluids, 33  
672 (2000), pp. 1027–1040.
- 673 [30] P. WESSELING, Principles of computational fluid dynamics, Springer Science & Business Media,  
674 2009.
- 675 [31] F. WHITE, Fluid mechanics, McGraw-Hill, 1994.
- 676 [32] X.HE, C.VUIK, AND C.M.KLAIJ, Block-preconditioners for the incompressible Navier-Stokes  
677 equations discretized by a finite volume method, Journal of Numerical Mathematics, 25  
678 (2017), pp. 89–105.